

TOPICAL REVIEW

Outdoor luminescence imaging of field-deployed PV modules

To cite this article: Oliver Kunz *et al* 2022 *Prog. Energy* 4 042014

View the [article online](#) for updates and enhancements.



You may also like

- [Addition of luminescence process in Monte Carlo simulation to precisely estimate the light emitted from water during proton and carbon-ion irradiation](#)
Takuya Yabe, Makoto Sasano, Yoshiyuki Hirano et al.
- [Cherenkov luminescence and PET imaging of ⁹⁰Y: capabilities and limitations in small animal applications](#)
Gregory S Mitchell, P N Thomas Lloyd and Simon R Cherry
- [Differences of the intensity increase of optical signals with fluorescein between Cherenkov-light and luminescence of water](#)
Seiichi Yamamoto, Takuya Yabe, Takashi Akagi et al.



TOPICAL REVIEW

Outdoor luminescence imaging of field-deployed PV modules

Oliver Kunz^{1,*} , Jan Schlipf², Andreas Fladung², Yong Sheng Khoo³, Karl Bedrich³, Thorsten Trupke¹ and Ziv Hameiri¹ ¹ University of New South Wales, Sydney, Australia² Aerial PV Inspection GmbH, Aachen, Germany³ Quantified Energy Labs (QE Labs) Pte. Ltd, Singapore

* Author to whom any correspondence should be addressed.

E-mail: oliver.kunz@unsw.edu.au**Keywords:** photovoltaic, characterisation, luminescence, photoluminescence, electroluminescence, solar power plantRECEIVED
14 July 2022REVISED
13 October 2022ACCEPTED FOR PUBLICATION
13 October 2022PUBLISHED
25 October 2022**Abstract**

Solar photovoltaic (PV) installations have increased exponentially over the last decade and are now at a stage where they provide humanity with the greatest opportunity to mitigate accelerating climate change. For the continued growth and success of PV energy the reliable inspection of solar power plants is an important requirement. This ensures the installations are of high quality, safe to operate, and produce the maximum possible power for the longest possible plant life. Outdoor luminescence imaging of field-deployed PV modules provides module image data with unparalleled fidelity and is therefore the gold standard for assessing the quality, defect types, and degradation state of field-deployed PV modules. Several luminescence imaging methods have been developed and some of them are already routinely used to inspect solar power plants. The preferred luminescence inspection method to be used depends on the required image resolution, the defect types that need to be identified, cost, inspection throughput, technological readiness, and other factors. Due to the rich and detailed information provided by luminescence imaging measurements and modern image analysis methods, luminescence imaging is becoming an increasingly important tool for PV module quality assurance in PV power plants. Outdoor luminescence imaging can make valuable contributions to the commissioning, operation, and assessment of solar power plants prior to a change of ownership or after severe weather events. Another increasingly important use of these technologies is the cost-effective end-of-life assessment of solar modules to enable a sustainable circular economy.

1. Introduction

Solar photovoltaic (PV) installations have been growing exponentially worldwide at an impressive compounded annual growth rate of about 43% [1] in the last decade. During this period, PV has emerged not only as one of the fastest-growing energy sources globally, but also as the cheapest form of utility-scale electricity in human history [2–6]. Arguably, therefore, PV is the most promising technology to supply the majority of the world's ever increasing energy demands [7–10]. Importantly, PV-generated electricity also provides humanity with the greatest opportunity to mitigate accelerating climate change by enabling the imperative energy transition away from fossil fuels to sustainable zero-carbon energy sources [1, 9–13], enabling living within the planetary boundary conditions [14].

PV power plants are required to operate reliably throughout their intended lifespan of 25 years or more [1, 15, 16]. Hence, solar modules are expected to operate for more than two decades in the field despite continuous exposure to constantly changing harsh environmental conditions, including high humidity, high UV exposure, strong thermal cycling, strong winds, corrosive air (in coastal regions), hailstorms, and more. All of these influences can cause damage to PV power systems [17–20]. This stringent longevity requirement imposes substantial challenges on the operation and maintenance of solar power plants, some of which currently comprise up to millions of solar modules. Additionally, defects in solar power plants may pose safety risks that must be identified and eliminated early for safe plant operation. For these reasons, it is

essential to monitor PV modules in the field regularly for performance degradation and safety. An explanation and summary of the most common PV module failure and degradation modes is provide in [21] and their associated economic impact is evaluated in [22]. It was found that cell cracks, potential induced degradation (PID) and short-circuited bypass diode failures have a total economic impact (in 2021) of about 6, 5 and 2 € kWh⁻¹, respectively, based on one year of defect time.

Another equally important matter relates to the profitability and economic risk mitigation of PV investments [23]. From a financial viewpoint, investors need efficient and reliable field inspection tools (and services) to identify any risk on future investment returns as early as possible [24]. Solar plant monitoring and inspection is therefore in increasing demand and will likely be indispensable to keep the rapidly growing number of PV assets in good health. To maintain financial risk within acceptable levels to investors and solar plant owners, it is therefore imperative to thoroughly inspect solar power plants (a) after the commissioning stage to ensure that modules have not been damaged during transport and installation; (b) prior to a change of ownership; (c) throughout the plant's lifetime to capture unacceptable degradation levels and safety risks; and (d) after severe weather events for damage assessment.

In addition to regular solar plant monitoring and inspections, the success of solar energy will also critically hinge on the availability of suitable, cost-effective, and accurate inspection methods to determine the best use of decommissioned PV modules (end-of-life assessment) to enable a thriving circular economy [25–29].

Fielded PV modules can suffer from a wide range of faults and degradation mechanisms that reduce their electrical output and lifetime [16, 22, 30]. Hence, fast and accurate identification of PV module failures has increasingly become a necessity [10]. A wide range of inspection methods exist and good overviews are provided by [28, 31]. Visual [11] and thermographic (infrared thermal) imaging [12] are commonly used for fast and cost-effective field inspection, the latter often by remotely piloted aircrafts (RPAs, drones) [13, 14]. However, visual inspection is insufficient to identify most electrical faults [9], while thermal imaging, especially when applied using drones, is limited in image quality and resolution [15]. Illuminated current–voltage (light I – V) measurements enable the assessment of power losses in PV arrays, strings, or modules in the field; however, they are not suitable for predicting future energy production and associated asset risks due to their limited ability to pinpoint the cause of the power loss. An optimal PV plant health assessment strategy will necessarily involve a range of different monitoring and inspection technologies, considering the strengths and weaknesses of different approaches together with the requirements of plant owners and operators [31]. In the near future, these inspection services will likely become progressively more automated [32, 33], with some of them completely autonomous [34, 35].

Inspection systems based on luminescence imaging have an important role to play in performing quality checks of solar power plants due to their ability to detect defects in solar panels with unparalleled accuracy and resolution [36, 37]. Figure 1 contrasts the luminescence-based technologies (i.e. electroluminescence (EL) and photoluminescence (PL) imaging) to other available imaging methods used for the defect detection and determination of faults and degradation (taken from [28]). While many imaging-based PV inspection technologies have been developed, it is evident from figure 1 that the luminescence-based technologies provide higher resolution image data compared to alternative methods. Furthermore, the fundamental advantage of luminescence images is the fact that the signal strength directly correlates with electronic performance (compare equation (1)). They are therefore capable of detecting a wider range of faults and with higher accuracy compared to non-luminescence-based methods. This paper aims to review the progress in luminescence-based imaging methods for field-deployed PV modules.

2. Luminescence imaging: technology and background

Luminescence in a semiconductor material is a process where an excited charge carrier transfers from a high energy state to a low energy state (electron–hole recombination) while the excess energy is emitted via a photon [38]. In this process, the luminescence intensity I_{PL} (number of photons per second per area) is directly related to the quality of the inspected semiconductor material, essentially the diode voltage V_{d} [39]. This can be expressed as

$$I_{\text{PL}} = Cn_i^2 \exp\left(\frac{V_{\text{d}}}{V_{\text{T}}}\right), \quad (1)$$

where C is a proportionality constant that is related to the optical properties of the sample, n_i is the intrinsic carrier concentration, and V_{T} is the thermal voltage (about 25.85 mV at room temperature) [40]. Therefore,

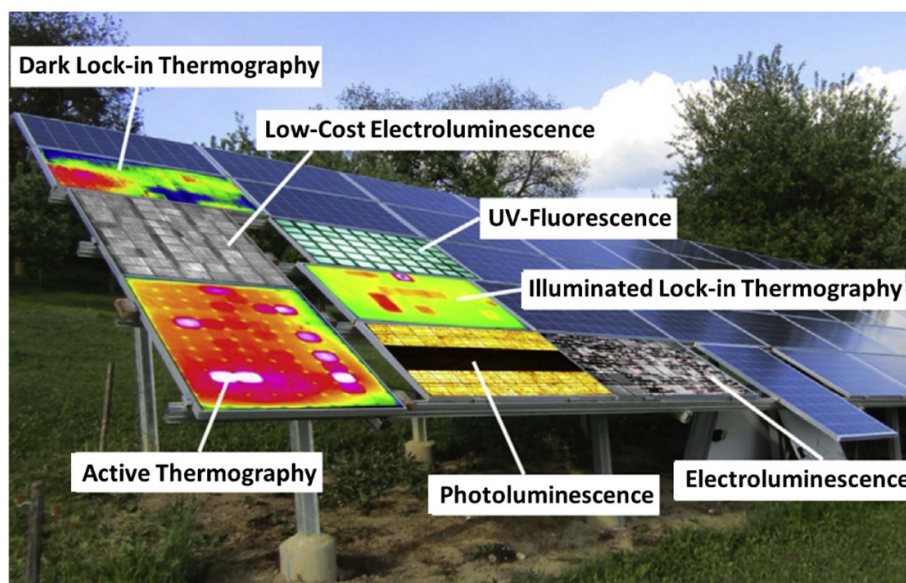


Figure 1. Various imaging-based characterisation methods for solar plant inspection of field-deployed solar modules. Reproduced from [28]. CC BY 4.0.

the luminescence intensity can be taken as a proxy for the local material quality. In other words, any imperfections (shunts, recombination centres, cracks, etc) that affect the voltage of a cell locally or globally can be identified using luminescence imaging. It is interesting to note that, compared to light $I-V$ measurements, which exhibit a strong voltage drop with increasing temperature (about 2.2 mV loss per $^{\circ}\text{C}$ increase for each cell in the module), there is only a very small dependence of the measured signal on the temperature in the case of silicon luminescence imaging [41]. This makes luminescence measurements ideal for outdoor conditions where typical module operating temperatures can routinely be above 50 $^{\circ}\text{C}$ [42].

As discussed, there are two types of luminescence imaging technologies that are widely applied in PV research and manufacturing [39]:

- EL imaging where excess charge carriers (electron-hole pairs) are created upon injection of a current into the device via suitable metal contacts [43], and
- PL imaging where the electron-hole pairs are created by photons that are incident on the device and absorbed in the semiconductor material [44]. The introduction of PL imaging by Trupke and Bardos in 2005 greatly extended the usefulness of luminescence imaging by allowing it to be applied not only to finished solar cells but also to solar materials at any stage in the production cycle (even to silicon bricks [45]), which has in turn revolutionised PV research and high-volume manufacturing [45, 46]. It is noteworthy to mention that the method has also recently been extended to allow imaging of entire PV modules in laboratory or fabrication settings using line illumination and a line scanning camera system [41, 47].

The EL and PL imaging techniques are equivalent in their ability to detect and locate electric defects, whereby defective or degraded areas appear dark in the images. Series resistance (R_s) related features show up in EL images as darker regions due to the voltage drop caused by R_s [48]. In PL images, R_s features can be identified using methods of current extraction, or via line-scanning PL [47, 49, 50].

Figure 2(a) displays a typical near infrared (NIR) luminescence signal from a silicon (Si) sample, ranging from about 1000 nm to 1300 nm and peaking at around 1150 nm [43]. A schematic of a typical PL and EL setup is displayed in figure 2(b). During PL measurements, the device is illuminated by a high-power light source (typically a laser or a light-emitting diode (LED)) and then subsequently emits a luminescence signal that is captured by a suitable digital camera. The resulting PL image can then be viewed and analysed via a computer. In the case of EL imaging, the light source is replaced by a power supply and the current is injected into the solar cell via its electrical contacts. EL imaging is based on the same process as LEDs with the distinction that a small amount of (infrared) light is emitted over a large area in the case of a solar cell, whereas for LEDs the light output (mostly visible) can be very large and is emitted from a very small area.

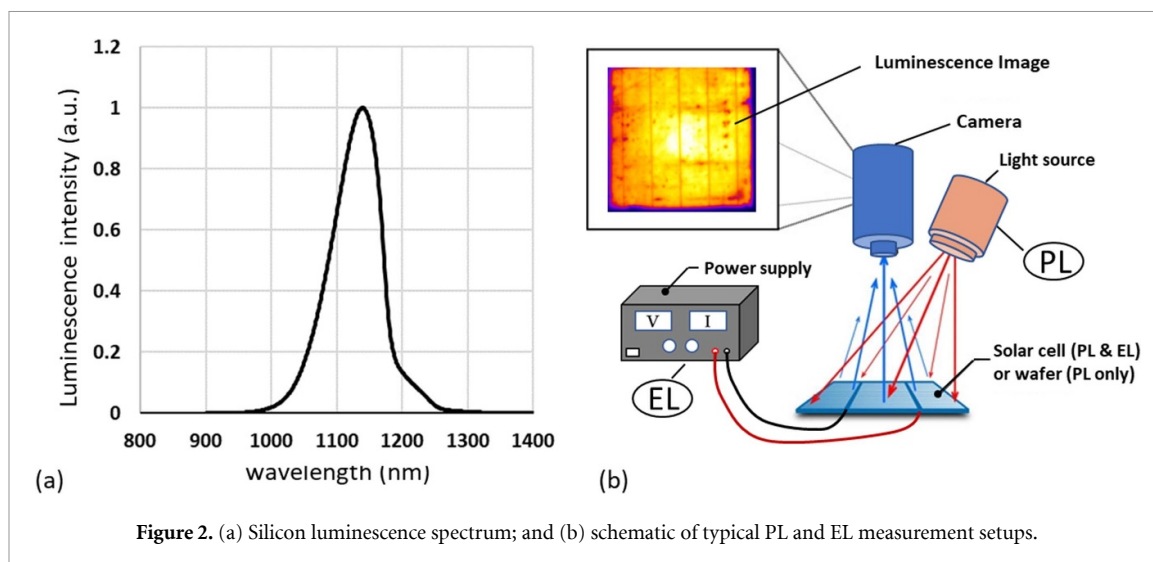


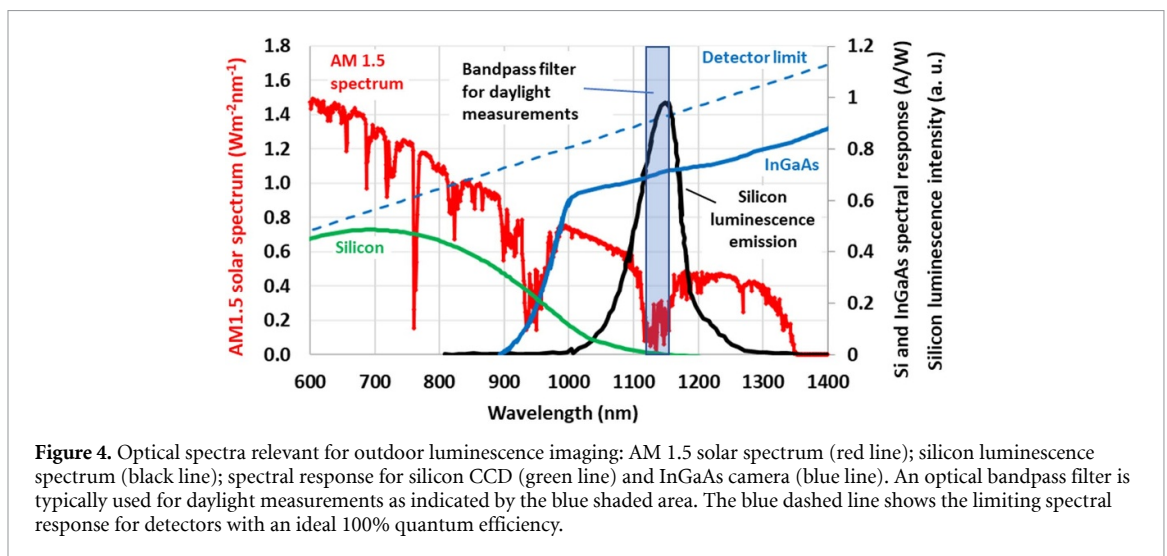
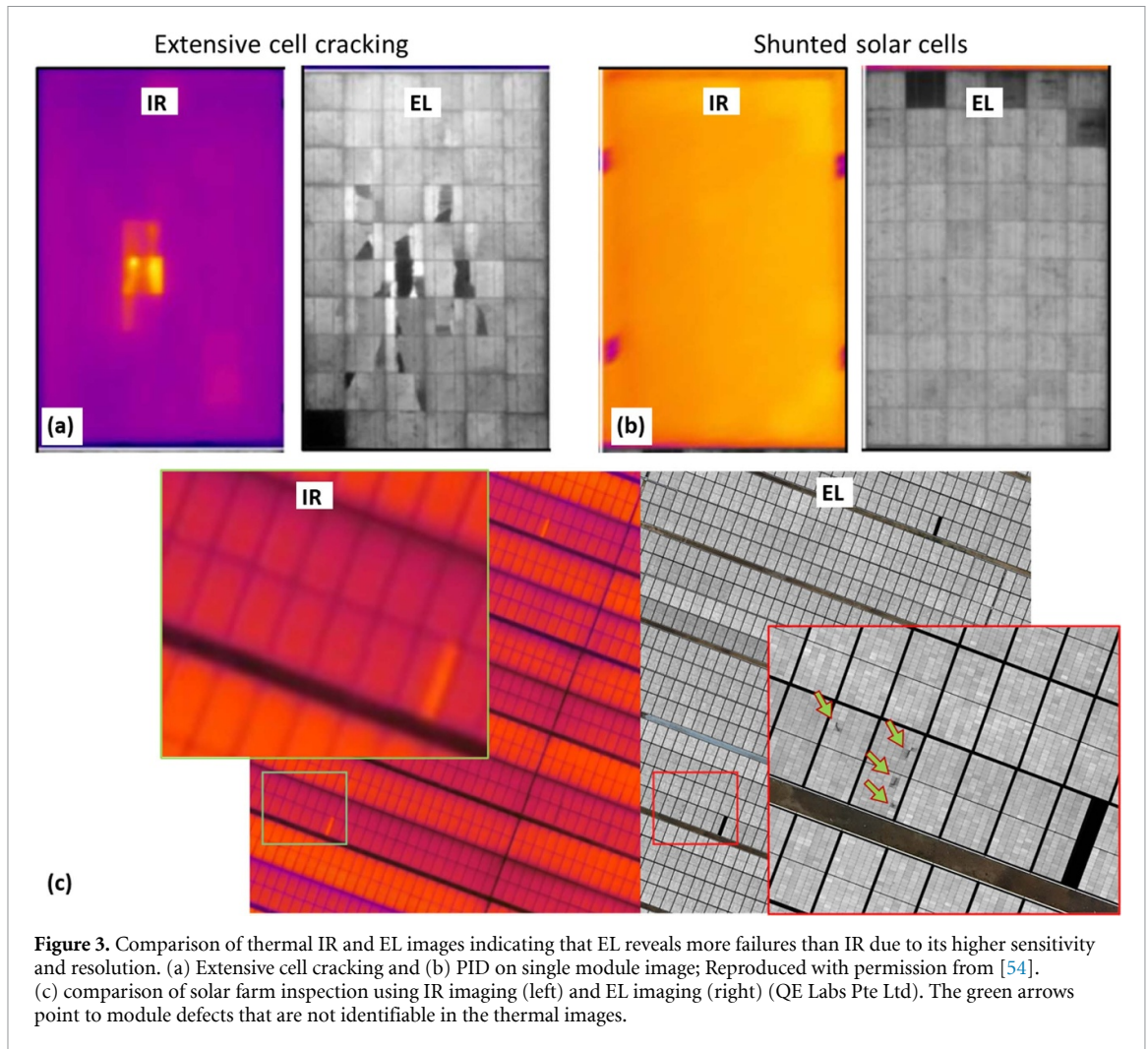
Figure 2. (a) Silicon luminescence spectrum; and (b) schematic of typical PL and EL measurement setups.

3. Specific advantages and challenges of outdoor luminescence imaging of fielded PV modules

In recent years there has been substantial interest in outdoor luminescence imaging of field-deployed solar panels. This has been pursued by research organisations [51–57] as well as commercial entities [54, 58–61]. Arguably, the main reason for this increased popularity is the ability of luminescence imaging to detect a large number of defects via high quality, high resolution image data [31, 54, 62]. For instance, figures 3(a) and (b) show a comparison between infrared (IR) images and the corresponding EL images of two fielded solar modules [54]. One of the modules suffers from extensive cracking and even some isolated cell regions (left) while the other module is affected by severe shunting (dark cells in the image), possibly from PID (right) [63]. Figure 3(c) further compares IR and EL measurements of a utility-scale solar farm. In this example, the IR imagery only suggests a bypass diode failure in a module, whereas the EL imagery also identifies additional defects such as backsheet scratches due to construction mishandling. From these images, one can conclude that EL has better capabilities to detect defects accurately and reliably compared to thermal IR. Despite this superior feature of EL, thermal IR imaging is currently the dominant image-based PV inspection technology in the market. The reason for this is mainly due to the capability of thermal imaging to capture substantially more data in the same period of time (higher throughput) compared to luminescence-based technologies [64, 65] leading to a comparatively low inspection cost [66]. Another reason for the popularity of thermal IR inspection is that the thermal IR cameras can be used for many different applications, ranging from the integrated circuit industry to energy efficiency and military applications. This has led to a wide range of commercially available thermal IR cameras and drone-mounted camera systems and subsequently the cost of these inspection systems has been falling substantially, while the maturity and capabilities of the technology have simultaneously improved.

There are also fundamental reasons why luminescence imaging (EL or PL) of fielded silicon solar panels is currently more difficult and time consuming than thermal IR: (a) for EL imaging the PV modules need to be disconnected from the PV system and (b) a suitable power supply (that requires a high power generator or grid connection) is needed to energise the solar modules or strings, (c) for daylight measurements the luminescence signal intensity is very weak compared to the strong sunlight interference, and hence, the solar modules or strings under test need to be modulated to extract the very weak luminescence signal in the presence of the very strong sunlight reflected from the module surface, and (d) expensive and less common indium gallium arsenide (InGaAs) cameras that feature a high quantum efficiency in the required wavelength region are needed for daylight luminescence or high throughput EL imaging at night.

Figure 4 displays various optical spectra that are relevant for outdoor luminescence measurements. For measurements during night-time, it is possible to use a suitable Si camera despite its low sensitivity (green line) in the wavelength region where Si emits luminescence signal (black line). This is only possible since there is no interference from the sunlight (air mass (AM) 1.5 spectrum, red line) which is typically about two orders of magnitude stronger than the luminescence emission from a solar module [53]. For daylight measurements, however, an InGaAs camera (blue line) is required due to its very high sensitivity in the 1150 nm wavelength region where Si emission is strongest [67]. While these cameras are typically much more expensive than their Si counterparts and feature lower spatial resolution (typical sensor resolution is



640 × 512 pixels compared to several megapixels for Si cameras), they have a spectral response that is close to an ideal photon detector, featuring an external quantum efficiency of 100% (blue dashed line). Note that the Si luminescence spectrum (black line) peaks roughly in the same region where the AM1.5 solar spectrum has a strong water vapour absorption band. This fortunate coincidence makes outdoor PL measurements substantially easier during daylight conditions when a bandpass filter with a centre wavelength of about 1140 nm and a width of about 25–50 nm is used (blue shaded rectangle).

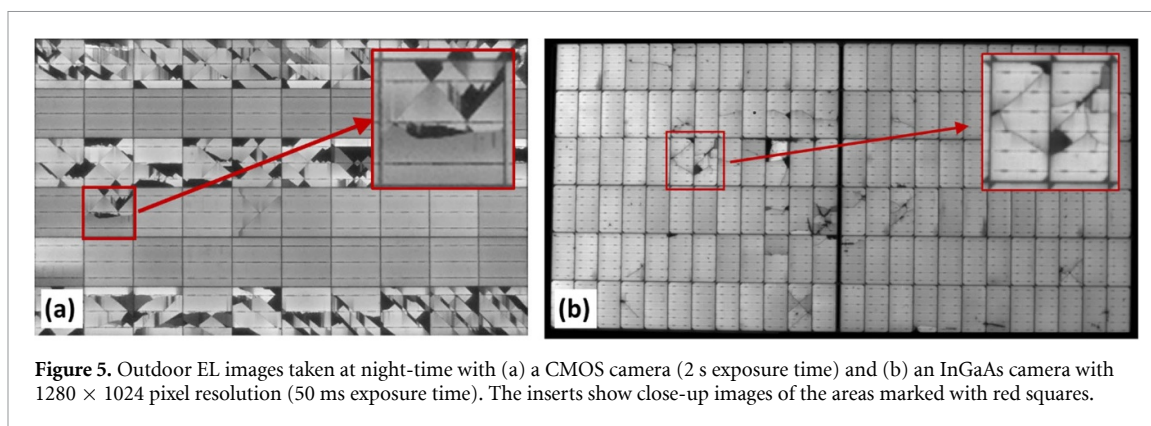


Figure 5. Outdoor EL images taken at night-time with (a) a CMOS camera (2 s exposure time) and (b) an InGaAs camera with 1280×1024 pixel resolution (50 ms exposure time). The inserts show close-up images of the areas marked with red squares.

4. Outdoor EL imaging at night

As discussed in the previous section, it is easier to perform luminescence-based measurements in the dark (at night). Under these conditions, it is possible to use low-cost commercial Si-based charged-coupled device and complementary metal-oxide semiconductor (CMOS) cameras, despite their much lower quantum efficiency in the relevant wavelength region around 1150 nm. An additional advantage of Si sensors is their much higher resolution, thereby enabling high definition EL images even when several modules are imaged simultaneously. Figure 5 compares high-resolution night-time outdoor EL images taken with (a) a Si camera and (b) a 1280×1024 pixel InGaAs camera. While figure 5(a) features a heavily cracked module with many electrically isolated areas, figure 5(b) displays a module with a variety of different features. The close-up inserts on both images show that for single module image acquisition, high definition EL images can be achieved with both types of cameras. While Si cameras are sufficient for most night time applications, it can be advantageous to use InGaAs cameras at night as well, for instance for older Si modules with low PL emission (see figure 6(c)) or to reduce motion blur when images are taken from a moving testbed [68, 69]. EL images generated from video-scans at a speed of multiple meters per seconds can be obtained due to the short exposure time offered by InGaAs cameras. An evaluation of different camera technologies with respect to EL image quality is provided in [70].

EL inspection is useful for the detection of various module faults including backsheet scratches (figure 6(a)), cell cracking (figure 6(b)), PID (figure 6(c)), and light- and elevated temperature-induced degradation [71]. Furthermore, high-resistance cell connections can be identified along with connection issues such as substrating failures, disconnected modules, and defective bypass diodes (BPD; in short-circuit mode). For comparison, figure 6(d) displays several PV modules imaged with a Si camera that do not display any significant defects.

A typical application of night-time (dark) EL imaging is the inspection of PV systems to identify yield losses or damage assessment after severe weather events like storms or hailstorms. In recent years, EL has also become increasingly popular for quality control during the commissioning stage of new PV installations to ensure module and plant integrity prior to operation or as part of PV monitoring and maintenance routines.

4.1. Technical specifications of the measurement systems

Various technical systems have been developed and are routinely used for night-time EL imaging. Ground-based solutions include single-camera mechanical mounts as in figure 7(a), multi-camera bridge systems (figure 7(b)), mobile units that use cranes (figure 7(c)), or ground vehicles fitted with EL cameras. Modified digital consumer cameras with CMOS sensors and lenses suitable for NIR imaging are often used with exposure times in the order of 1–2 s for an individual EL image.

Drones (figure 8(a)) fitted with similar CMOS cameras and lenses can also be employed for dark EL recordings. Due to the large weight of the cameras, current EL drone systems have a total weight of around 10 kg. Legal regulations for the operation of these drones for night-time flights vary between countries, but usually require specific permits and highly trained drone operators. Since it is generally difficult to take sharp single EL images, EL videos are typically recorded. The drone is moved by stop-and-go along the module rows. This facilitates typical recording frequencies of up to 25 frames s^{-1} . An alternative drone-based system for night-time EL imaging uses high sensitivity InGaAs cameras (figure 8(c)). Such drone EL systems may be lighter due to a comparably smaller camera sensor and lens size. As InGaAs cameras are capable of capturing images at short exposure of the order of a few milliseconds, drones equipped with them are able to

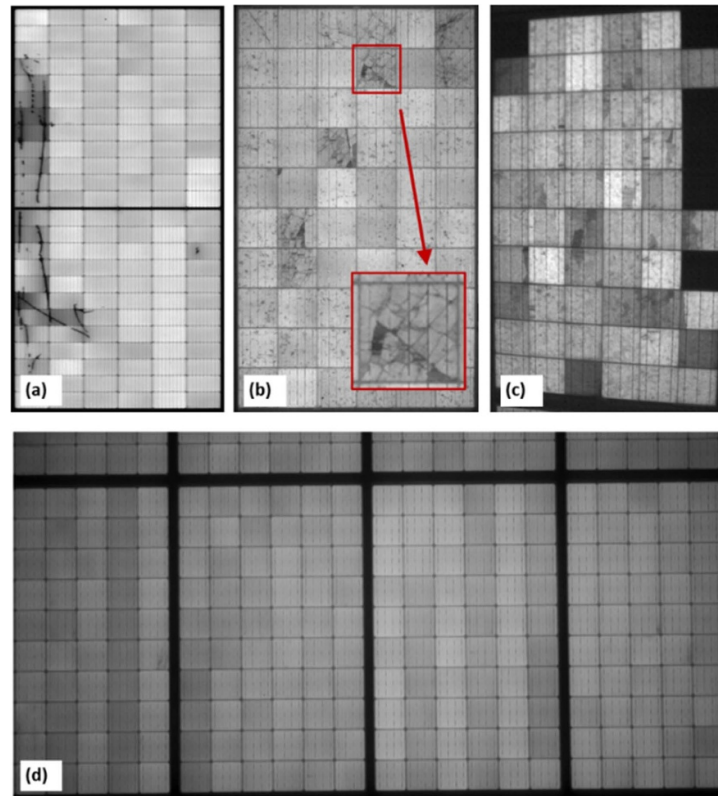


Figure 6. Night-time EL images of PV modules with different defect types: (a) half-cell mono-crystalline Si module with backsheet scratch; (b) multi-crystalline module with heavy cell cracking; and (c) ten year-old multi-crystalline Si module with strong PID (taken with an InGaAs camera due to the very low luminescence signal). The modules in (d) were imaged simultaneously and do not feature any significant defects.

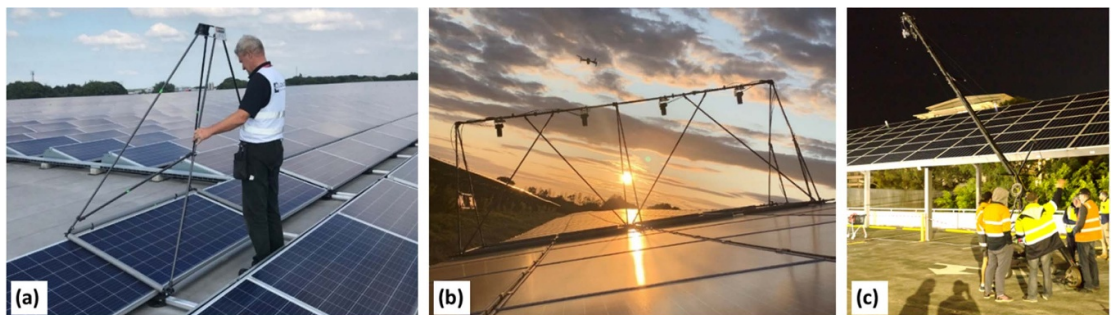


Figure 7. Commercial dark EL measurements carried out (a) using a single-camera system on a rooftop, (b) a multi-camera bridge system in a utility-scale PV power plant (aerial PV Inspection GmbH), and (c) a camera crane on a car park roof installation (UNSW).

continuously scan the PV string while recording videos. Flying drones at a constant speed across solar installations (instead of stop-and-go operation) is more effective since it saves battery life and substantially increases the imaging throughput. Advanced image-processing techniques can subsequently be utilised to extract single module images from the video recordings (see figures 8(b) and (d)).

The selection of a measurement system is primarily determined by the PV installation layout, the required resolution, and the purpose of the inspection. Some tasks such as the assessment of micro-cracks, require high-quality single module images that currently can be achieved only with stationary ground-based systems (tripod/bridge/crane). On the other hand, some tasks require high volume inspection in a limited amount of time and fast evaluation of major defects, making drone EL systems a good choice. In addition, some PV installations, such as compact module arrays on roof-tops, façades, and floating installations, can only be inspected with drones.

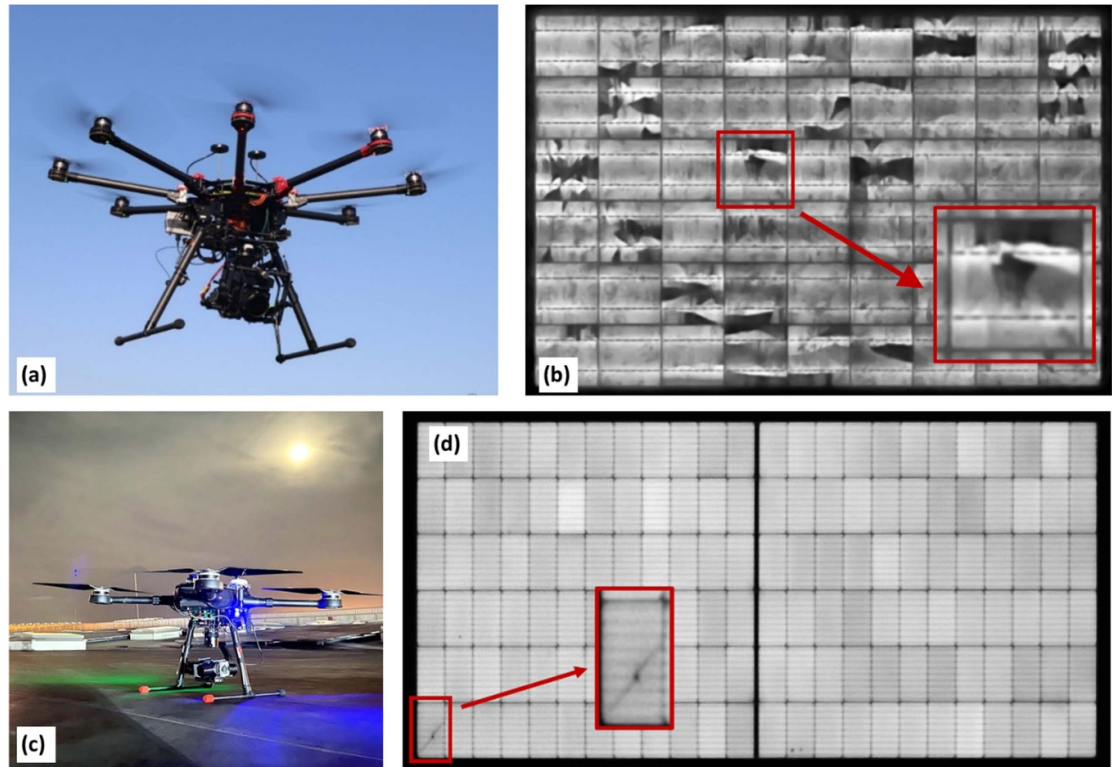


Figure 8. (a) Silicon camera-based drone EL system used for video recordings and (b) a corresponding module EL image extracted from a video recording (aerial PV inspection GmbH). The insert in (b) shows a close-up image of the area marked with a red square. (c) InGaAs camera-based drone EL system used for video recordings and (d) a corresponding processed module EL image using multiple-frame averaging algorithm (QE Labs Pte Ltd). The insert in (d) shows a microcrack due to a point impact.

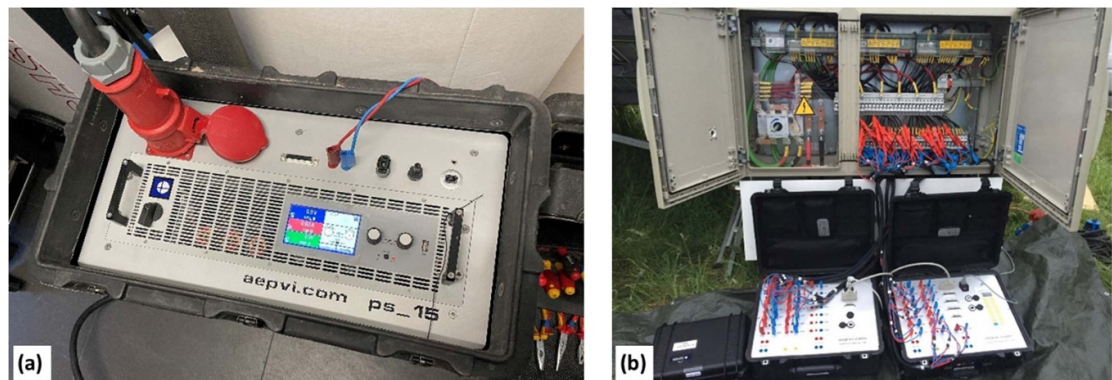


Figure 9. Equipment required for measurements of PV strings: (a) 15 kW, three-phase string power supply, and (b) combiner box with a multiplexer switch and required cable connections [54].

4.2. Technical specifications of the power supplies

The biggest current challenge for fast EL measurements is the power supply that is required to energise the PV string. With the typical modern modules of 400–500 Wp and strings of up to 30 modules, power supplies >15 kW are needed to power one PV string. Typically, the current applied in EL measurements is in the range of 0.5–1 times the short-circuit current of the modules. Therefore, a suitable DC power supply unit needs to be programmable with specifications of 0–15 A, 0–1.5 kV, and 0–15 kW (see figure 9(a)) [72]. The power supply itself is powered by either a three-phase grid connection or a mobile petrol generator that needs to be carried to the PV installation. This limitation may change in the future as some inverter manufacturers are developing new inverters that can provide power to individual strings [73], which has the potential to significantly speed up EL inspections and thereby reduce their cost. Note that if only a small number of modules need to be measured in the field, they are often disconnected from their strings and plugged into a battery-powered DC supply with much more relaxed specifications of only about 900 W (15 A and 60 V).

To increase throughput and reduce costs of night-time EL imaging, high-power multiplexer-switch systems which connect up to 100 strings to a power source can be used (see figure 9(b)). The required wiring is typically done prior to measurements to avoid the need for re-wiring in the dark. During the measurements, the power is switched from string to string via remote control. The connection of the multiplexer-switch systems to the PV installation requires an electrician with special certifications.

4.3. EL inspection workflow and throughput

Typically, the EL measurement systems are prepared onsite during the day and configured to the size and layout of the modules to be measured. Around dawn, when the power produced by the PV plant is very low, the electrical preparation is done, i.e. connecting all strings to be measured to the multiplexers and power supplies. Dark EL measurements then start at very low light levels. In the case of bridge systems, two people are needed for moving the mounting system around. During the measurements, it is important to continuously monitor the image quality and to record the module location with each image.

Inspection throughput mainly depends on the number of strings connected to the power supply, the plant layout, the accessibility of the PV installation, and the targeted image quality. Approximately 1500–3000 modules (corresponding to about 550 kW–1.1 MW) can be imaged per night using multi-camera bridge systems for single module imaging. Bridge systems with up to eight cameras have been deployed successfully to increase the measurement throughput.

In the case of silicon camera-based drone EL inspection, where single module EL images are extracted from the recorded videos, about 150–300 modules can be inspected per drone per hour. This includes the time required for swapping the drone batteries after exhaustion since the drone battery lasts for only about 20 min on a single charge. With increased flight speeds, much faster image acquisition is possible at lower image quality, which is sufficient for PID detection but not for the detection of small features. For an InGaAs camera-based drone EL system, about 1200–1500 modules per hour or an average of 12 000 modules EL inspection per night has been demonstrated on the full-site EL inspection of 60 MW floating PV project [74]. The speed is made possible through imaging a short exposure times (<5 milliseconds), automated route planning based on the site layout, and autonomous drone piloting and scanning of PV strings [74]. Research on improving the efficiency of these automated drone flight systems to take EL images is ongoing [32].

EL is a powerful inspection tool to uncover many PV modules faults during production, transportation, installation, etc. It is especially useful at certain milestones of PV plant's 25 year lifetime such as the initial site acceptance test after the completion of system construction, the final acceptance test before the end of the defect liability period, preventive maintenance before the end of product warranty provided by the module manufacturer, etc. For projects where cost is a constraint, EL inspection can be done on a sampling basis. There are available standards such as the ISO 2859-1 that help to determine the required sampling rate [75]. Depending on the inspection purpose and sampling criteria, the sample rate can be in the range of 1%–20%.

5. Daylight luminescence imaging methods

5.1. General requirements

As mentioned above, a core requirement for all daylight luminescence-based imaging methods of Si solar modules is that an InGaAs camera and suitable optical filtering are used. The most widely used InGaAs cameras now feature image sensors with a resolution of either 640×512 pixels or 1280×1024 pixels. Apart from one exception (see section 4.4 below), a second requirement is that multiple images are taken at different modulation points (lock-in approach), that is

- (a) a 'High' state where a large number of electron–hole pairs recombine within the solar cells (a certain fraction of this recombination is radiative, i.e. emitting luminescence signal; hence, high PL signal), and
- (b) a 'Low' state where significantly less radiative recombination takes place (low PL signal).

In the case of outdoor PL imaging, a typical modulation could, for instance, involve switching the solar modules from open-circuit (OC) to the maximum power point (MPP) in rapid succession and taking a single image at each modulation stage. Typical timing for such an image acquisition process is illustrated in figure 10(a) where images that are taken at the 'High' modulation state feature both luminescence signal and the reflected ambient sunlight, while those taken at the 'Low' modulation state show mostly ambient light and only negligible luminescence signal. To achieve the required high signal-to-noise-ratio (SNR), the process is usually repeated several times (see figure 10(b)). The final outdoor luminescence image is then calculated by subtracting the average of the Low-state images from the average of the High-state images, a procedure that largely removes the ambient reflected sunlight. Because of the strict timing requirement of this approach, the switching between the modulation states and image acquisition needs to be carefully

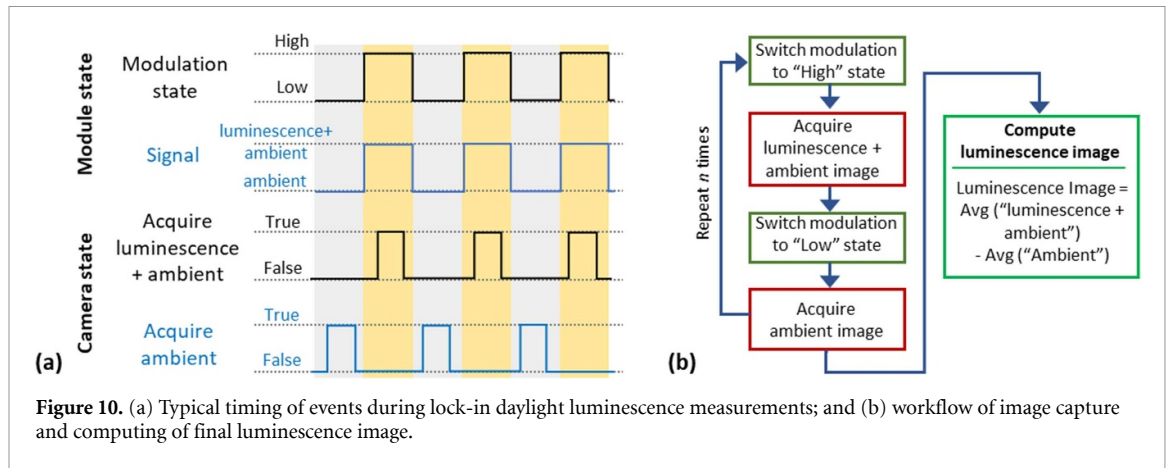


Figure 10. (a) Typical timing of events during lock-in daylight luminescence measurements; and (b) workflow of image capture and computing of final luminescence image.

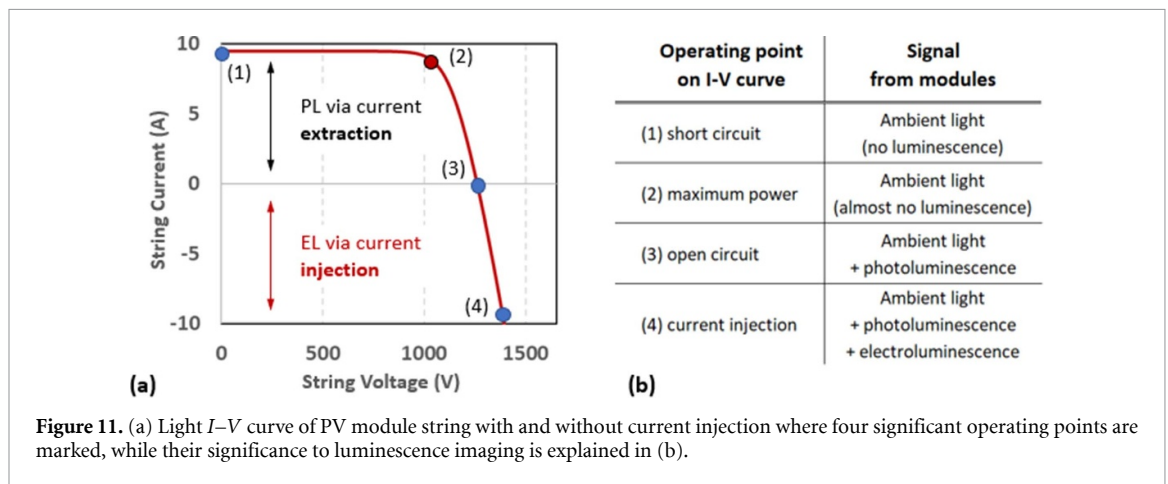


Figure 11. (a) Light I–V curve of PV module string with and without current injection where four significant operating points are marked, while their significance to luminescence imaging is explained in (b).

synchronised. However, in cases where such synchronisation is impractical or impossible, another workflow sequence, ‘batch acquisition’ [76], can also be used. In the batch acquisition procedure, a series of images is taken at each state and the modulation state is switched *only once*, e.g. from Low-state to High-state. This switching point can be detected by analysing the image sequence. Subsequently, an outdoor PL image can be computed by an equivalent subtraction process as presented in figure 10(b).

5.2. Outdoor luminescence imaging in daytime using electrical modulation

Currently, the most common approach to take outdoor luminescence images in daytime is to use an InGaAs camera with suitable optical filtering in combination with electrical modulation (based on the lock-in principle). Electrical modulation is based on connecting specialised equipment to individual modules or to entire module strings via the module terminals [57, 61, 77]. This typically requires a licenced electrician and adherence to specific safe working procedures since high voltages (up to 1500 V) and arcing can be very dangerous when connecting and disconnecting energised PV module strings. There are different possibilities for electrical modulation as indicated in figure 11(a), the light I–V curve of a PV module string in normal operation (top half of the curve) and with current injected at the terminals via a suitable power source (bottom half of the curve). The working points indicated on the I–V curve are (see figure 11(b)): (a) short circuit, where essentially no luminescence signal is emitted from the PV module, (b) MPP, where almost no luminescence signal is emitted from the PV module, (c) open circuit, where the maximum of PL emission is reached, and (d) current injection, where PL and EL are present simultaneously. The dominating signal captured by the InGaAs camera, in all cases, is the reflected ambient sunlight. Thus, to extract luminescence images, the modules need to be toggled between two of these four points and extraction of the luminescence signal can then be achieved using a lock-in approach as explained above. Other points on the I–V curve between (a) and (d) can also be used, but in this case, a significant amount of power is extracted and needs to be dissipated, making the corresponding equipment bulky and expensive.

The principle of electrical modulation has been used routinely by Solarzentrum Stuttgart in their DaySy system [58, 61, 78] which is composed of (a) the DaySyCam and (b) the DaySyBox. The DaySyCam is an InGaAs camera that works at a frequency controlled by the DaySyBox. The DaySyBox has two operation

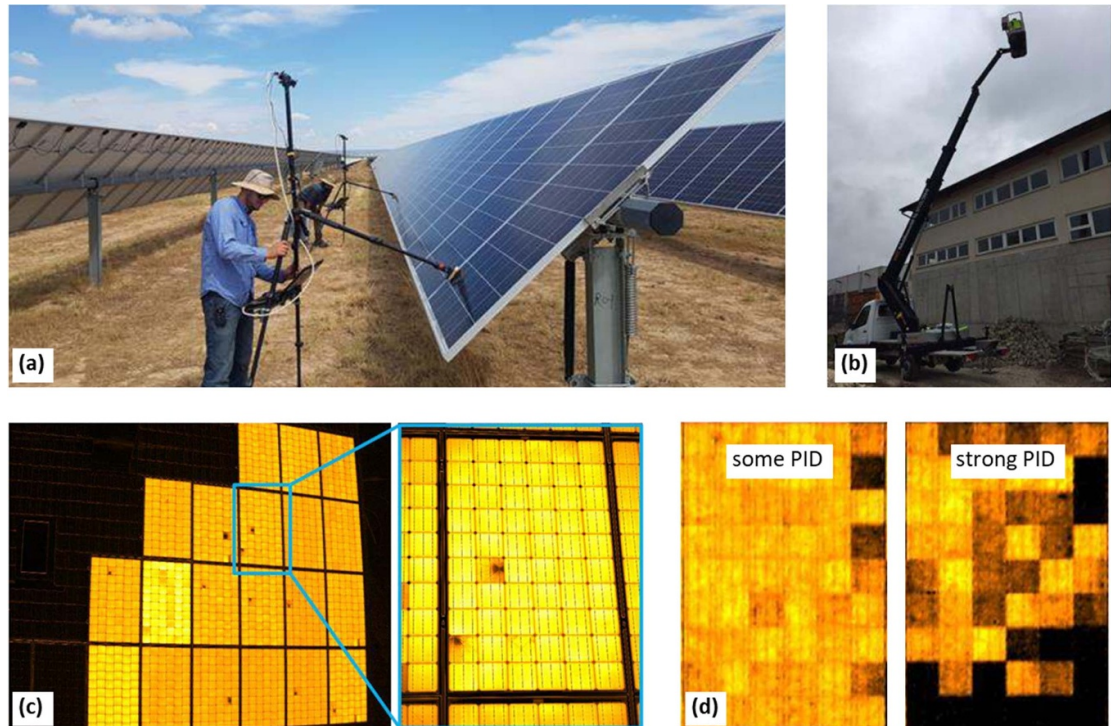


Figure 12. Outdoor luminescence imaging of (a) a utility-scale solar plant using two DaySyCams; and (b) a rooftop system with difficult access requiring the use of a basket crane vehicle. Outdoor luminescence images of (c) an entire PV string (increased throughput); and (d) two modules with different levels of PID. Reproduced with permission from [31]. IEA PVPS task 13.

modes where the power is fed into the PV string via either (a) up to six generator strings or (b) an external power source (typically a three-phase power supply with a generator). During the measurements, the DaySyCam is moved from module to module to acquire the images. Once all modules of a string are imaged, the DaySyBox is switched to a different target string and the procedure is repeated.

When performing luminescence imaging in the field, the camera placement prior to image acquisition is one of the most time-consuming aspects. On solar plants, this typically involves a tripod (see figure 12(a)) or other lightweight mechanical structure that holds the camera steady during image capture. For the inspection of rooftop systems, scissor lifts or basket cranes (figure 12(b)) can be used if the roof is not directly accessible or walkable. As discussed above, the measurement throughput depends very strongly on the required resolution. For the detection of micro-cracks, each module needs to be imaged individually. On the other hand, for the detection of large defects (like PID), it is possible to image entire strings of modules at once, hence, a significantly increased throughput. PV string imaging is illustrated in figure 12(c) also displaying a close-up image of one of the modules highlighted with the blue rectangle. An image of two PID-affected modules is displayed in figure 12(d) where the module on the left is mildly affected by PID and the module on the right has strongly degraded from PID.

In contrast to indoor module imaging, such as in a laboratory or manufacturing setting, every outdoor luminescence inspection is different in terms of access, setting, and throughput. As a guideline, the DaySy system can image about 500–700 kW_{peak} per day on a utility-scale solar plant when individual module images are taken [31]. One way of reaching such a high throughput is to simultaneously use multiple DaySyCams on a modulated PV string.

A completely different approach to taking outdoor PL images of PV modules in operating power plants was recently proposed by Vuković *et al* [79], where the electrical modulation is produced by a Wifi signal that controls the PV inverter (see schematic in figure 13(a)). This approach has the advantage that access to the PV string terminals is not required, which simplifies the imaging process and substantially reduces its cost. In a proof-of-concept study, the authors were able to take outdoor PL images (see figure 13(b)), however, the very slow switching frequency of the inverter posed major limitations on image quality and throughput. For instance, in this test, it took 27 s to acquire a single PL image, a time scale that is too slow for commercial applications. This time scale is also problematic due to the typically rapid fluctuation in outdoor light intensity. However, with further technological improvements or specifically designed inverters, this approach has the potential to become useful for both utility-scale and solar rooftop applications.

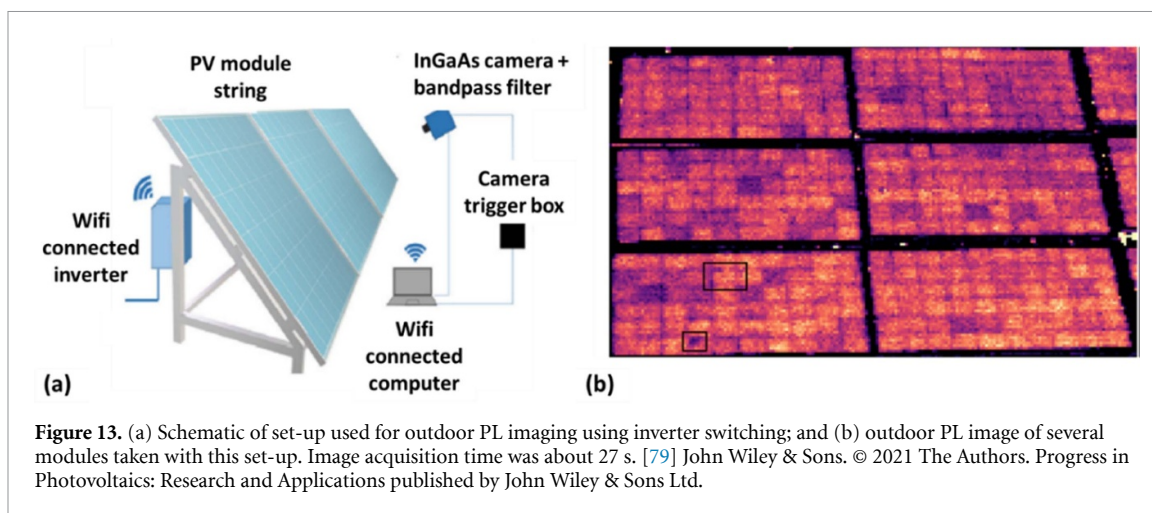


Figure 13. (a) Schematic of set-up used for outdoor PL imaging using inverter switching; and (b) outdoor PL image of several modules taken with this set-up. Image acquisition time was about 27 s. [79] John Wiley & Sons. © 2021 The Authors. Progress in Photovoltaics: Research and Applications published by John Wiley & Sons Ltd.

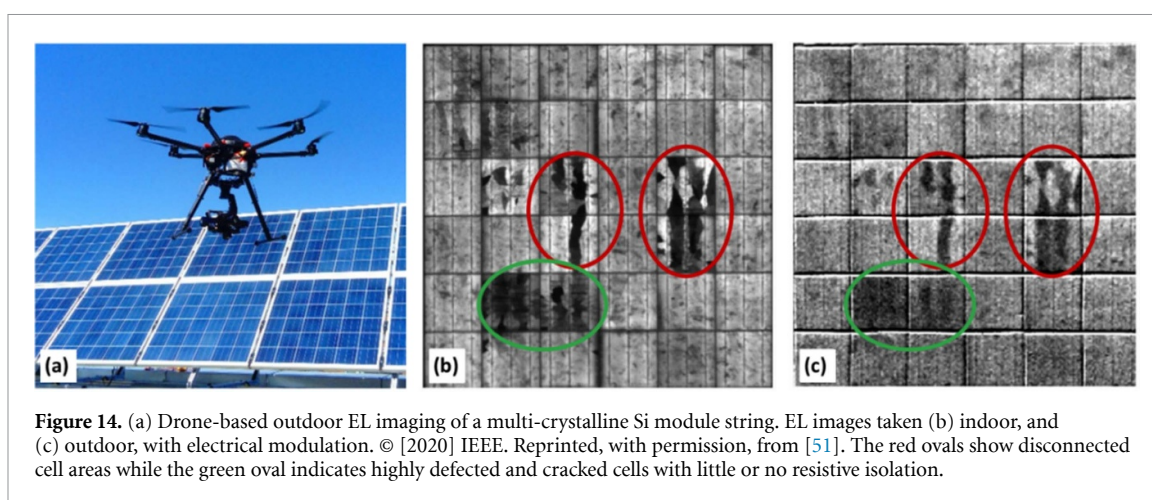


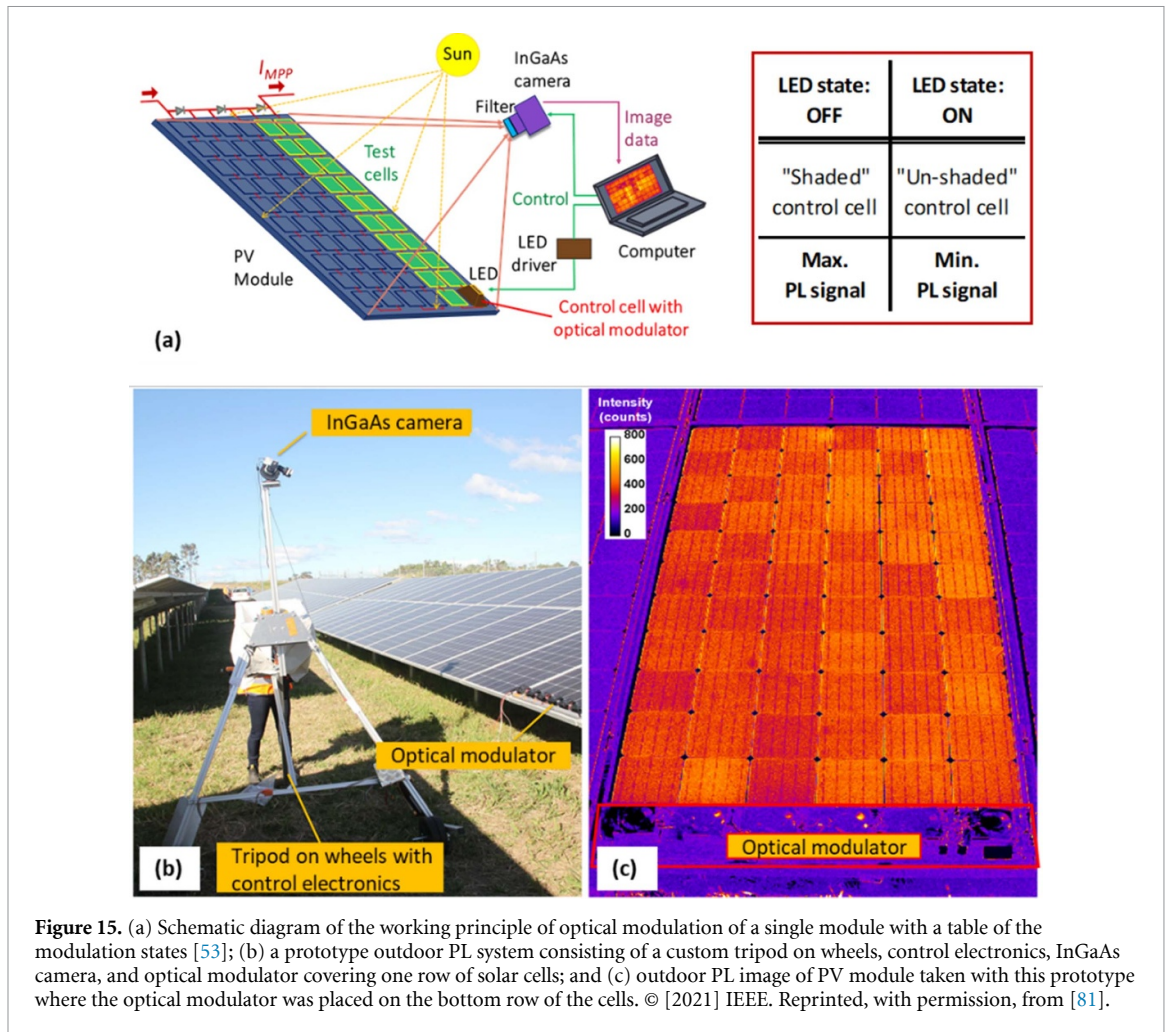
Figure 14. (a) Drone-based outdoor EL imaging of a multi-crystalline Si module string. EL images taken (b) indoor, and (c) outdoor, with electrical modulation. © [2020] IEEE. Reprinted, with permission, from [51]. The red ovals show disconnected cell areas while the green oval indicates highly defected and cracked cells with little or no resistive isolation.

Taking outdoor EL images with a short acquisition time is a core requirement if images are to be taken from drones as demonstrated by Benatto *et al* [51, 80], who performed drone-based daylight EL imaging of PV modules where an InGaAs camera with a high frame rate of $120 \text{ frames s}^{-1}$ was used. To limit the motion blur of the images, a short exposure time was selected (around 5 ms with video stream recording). The images were captured and stored on a drone-embedded computer and then post-processed to extract the PL images of individual modules from the video sequence. Figure 14(a) displays the hexacopter drone with the 640×512 -pixel InGaAs camera hovering in front of the module string under test. A comparison between indoor (figure 14(b)) and outdoor (figure 14(c)) EL images of the same multi-crystalline Si module reveal that resistively disconnected areas (red ovals) are easily identified in both images, but highly cracked areas (green ovals) appear as generally dark cells in the outdoor image due to the reduced image resolution. Further work is required to improve the image quality. Although the drone-based outdoor luminescence approach promises fast image acquisition of modules, its current requirement for physical electrical connections to the module strings (for electrical modulation of the modules) limits the measurement throughput.

5.3. Outdoor PL imaging in daytime using optical modulation

The previous sections discussed outdoor luminescence imaging (EL and PL) where the modulation is done via electrical connections. An alternative approach is toggling of solar modules between OC and short-circuit (or MPP) using a method known as ‘contactless switching’ via ‘optical modulation’ as introduced by Bhoopathy *et al* [53, 76]. Contactless switching refers to the fact that access to the module/system terminals is not required while optical modulation means that the PV modules are toggled between different states by strategically ‘shading and un-shading’ parts of the system. This approach requires only a battery-powered optical modulator.

The working principle of optical modulation can be understood from figure 15(a) which displays a single PV module with 60 individual cells that are grouped into three sub-strings, i.e. units of series-connected cells with one parallel-connected BPD. In normal operation, the MPP current (I_{MPP}) is extracted from the



module. However, when one cell (designated the 'control cell') in a sub-string is shaded, it limits the current flow in the corresponding sub-string. In this case, the other cells (green 'test-cells' in figure 15(a)) have a reduced current flow, which forces their operating point to approximately OC. The control cell can be 'shaded' and 'un-shaded' by LED-based optical modulator.

In essence, the LED array (optical modulator) controls the optical generation rate in the control cell, and hence, the emitted PL signal from the test cells. The use of LED arrays for this purpose is advantageous since LEDs can be turned ON and OFF in a highly controlled and rapid manner, which enables synchronisation with image acquisition and therefore, short overall PL image acquisition times of approximately one sec per image. The light intensity of the used optical modulator is slightly above one Sun intensity to ensure that the control cell does not limit the current flow when the optical modulator is turned ON. The table 1 in figure 15(a) displays the two states that can be toggled with the optical modulator. In practice, rather than one control cell, an optical modulator covering six control cells (or 12 half control cells in the case of half-cell modules) is chosen since this enables taking outdoor PL images of the entire module apart from the control cells (see figures 15(b) and (c)). Hence, to image the full module, a second PL image needs to be taken with the optical modulator in a different position (or three images in the case of half-cell modules). The composite of the individual PL images then produces the final outdoor PL image. This method has an approximate throughput of about 1–2 modules per minute and has recently been extended to allow diagnosis and quantification of series resistance effects as well as the identification of BPD that have failed in an OC condition [76].

The contactless outdoor PL imaging method can be significantly improved when applied to utility-scale PV power plants where many PV strings (up to 30 modules connected in series) are parallel-connected in an array resulting in large currents, often in excess of 2 kA, being fed into a central inverter, as schematically illustrated in figure 16(a). In this case, the 'optical PV string modulation' technique [81] can be used where four or five optical modulators are placed on PV modules of the same string (see figure 16). When the modulators are turned OFF, the respective 'control modules' are bypassed and their voltage drops from the

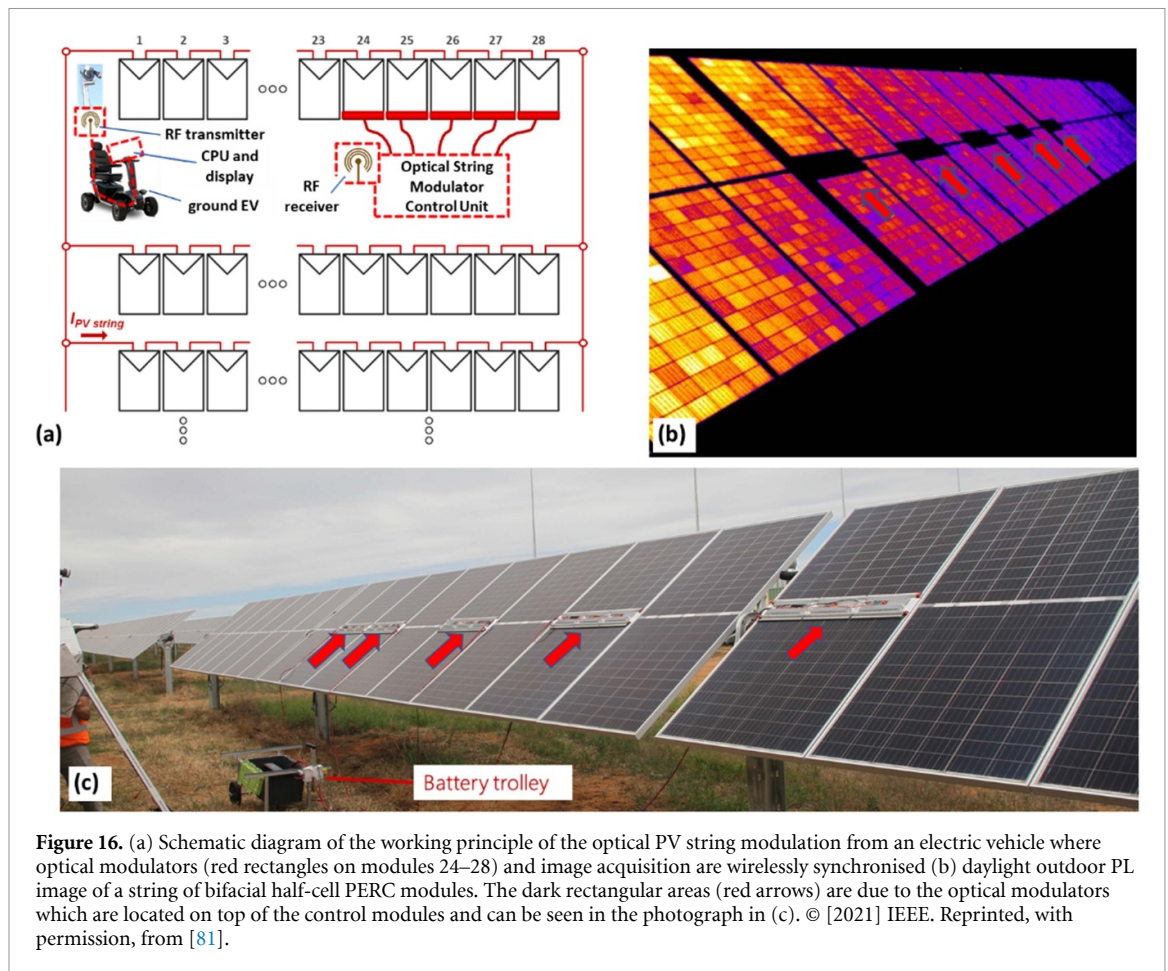


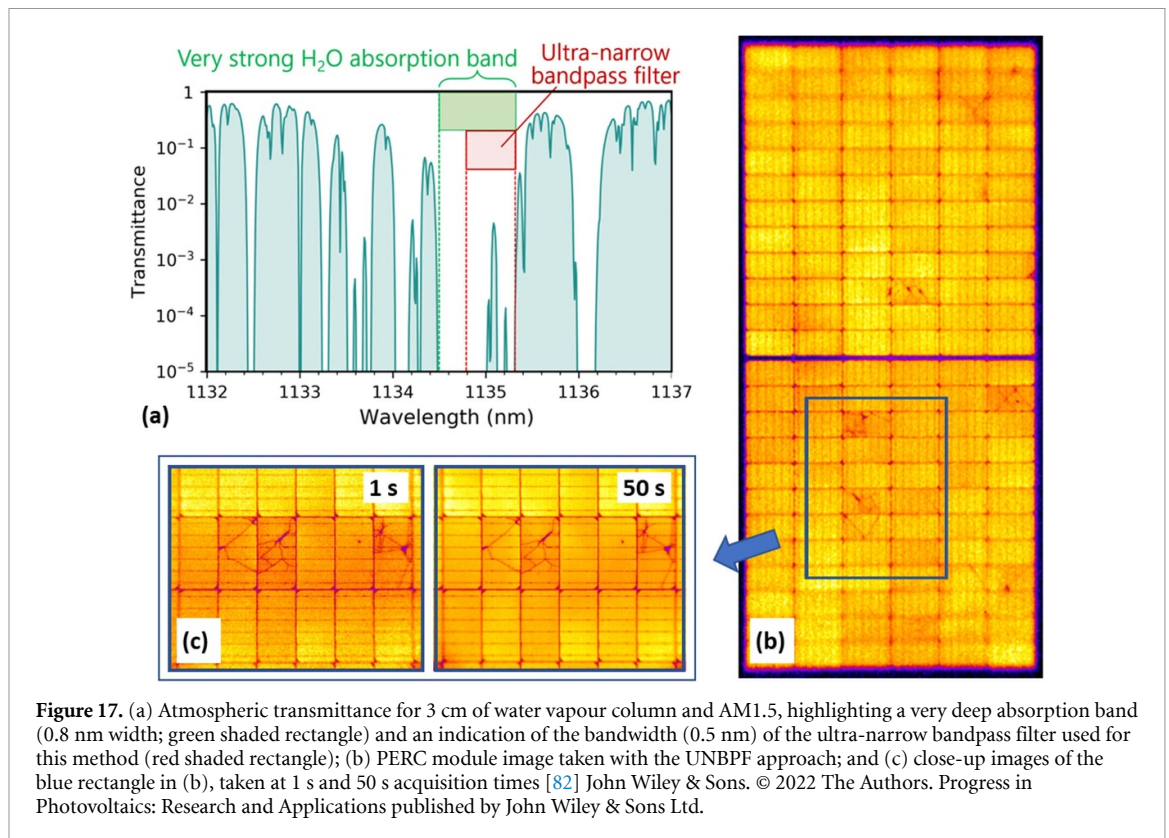
Figure 16. (a) Schematic diagram of the working principle of the optical PV string modulation from an electric vehicle where optical modulators (red rectangles on modules 24–28) and image acquisition are wirelessly synchronised (b) daylight outdoor PL image of a string of bifacial half-cell PERC modules. The dark rectangular areas (red arrows) are due to the optical modulators which are located on top of the control modules and can be seen in the photograph in (c). © [2021] IEEE. Reprinted, with permission, from [81].

MPP voltage to approximately zero (slightly negative due to the current flow in the BPD). Since the toggled string operates within a large array, the string's voltage remains constant and therefore, the other modules (the 'test modules') need to increase their voltage to compensate for the missing voltage of the control modules. For large scale plants, four to five optical modulators are required to shift the operating point of the test modules from MPP to OC. It is worth mentioning that other operating points (between MPP and OC) can also be achieved conveniently by toggling only some of the optical modulators in the system, which allows, for instance, the detection of series resistance-related features. A scenario where optical string modulation is particularly desirable is the fast screening of PV systems since many modules can be imaged at the same time (as in figure 16(b)). Detailed images only of modules of interest that show signs of degradation or damage can then be acquired. For an optimised workflow and throughput, two operators are ideal to move the optical modulators from string to string, one moving the image capture unit and the second moving the string modulators.

The main advantages of outdoor PL imaging via optical PV string modulation are:

- There is no longer a need to take multiple images of the same PV module;
- Four to five optical modulators switch a large number (up to 30) of PV modules, leading to significantly reduced manual handling;
- Images can be taken of more than one module at the same time (see figure 16(b)) which allows a substantial increase in throughput where about eight to ten modules can be imaged per minute (about 200 kW per hour).

Compared to daylight outdoor luminescence imaging via electrical modulation, optical string modulation has the main advantage that it removes the need to interfere with the electrical connections of the inspected PV power plants, meaning that no certified electrician is required. This not only reduces cost but also simplifies the measurements and increases the throughput. The contactless nature allows very easy movement of the equipment around to different locations in the solar power plant to obtain a statistically significant set of images. On the other hand, a potential drawback of outdoor PL imaging without an external excitation source is that the sun is the only power source; hence, it is challenging to image modules at low illumination levels. For passivated emitter rear cell (PERC) modules, for instance, it is ideal to have at



least 300 W m^{-2} insolation to achieve images with good SNR levels in an acquisition time of about 0.5–1 s. The general trend is that lower illumination levels reduce the SNR for outdoor PL while increasing the SNR in the case of electrical modulation.

5.4. Outdoor PL imaging in daytime without modulation

Outdoor luminescence imaging in daylight using electrical or optical modulation is well suited for detailed inspection of a large number of modules. In both cases, modulation is achieved via additional equipment that needs to either be connected manually (electrical modulation) or placed onto the modules (optical modulation). Importantly, both methods have one drawback in common—they require toggling of the modules' operating point and image acquisition in a lock-in mode. The method described in this section—outdoor PL imaging via ultra-narrow bandpass filter (UNBPF)—on the other hand, does not require toggling of the operating point but enables image acquisition in the manner of an ordinary 'point-and-shoot' digital camera [82]. The principle behind this method relies on a very strong water vapour absorption band where almost no sunlight reaches the Earth's surface. This can be seen from the atmospheric transmittance data in figure 17(a), based on the AM1.5 and a water vapour column of 3 cm. The absorption band (green shaded rectangle) has a very narrow width of only 0.8 nm but is, fortuitously, located around a wavelength of 1135 nm, where the PL emission from Si is high. With the use of an UNBPF (0.3–0.5 nm width; red shaded rectangle), it is possible to capture a PL signal from a PV module exposed to bright daylight that contains almost no ambient reflected sunlight.

While this appears simple in principle, it requires a 50–100 times narrower filter than what is used in other daylight luminescence methods. This pushes the limits of current filter manufacturing technology and leads to additional challenges arising from the angular dependence of the filter properties, since imaging applications involve a large variety of angles of incidence onto the optical elements used. Hence, a sophisticated custom-designed optical imaging system is required for this approach to work.

Figure 17(b) shows an outdoor PL image of a PERC module that was taken using the UNBPF-based outdoor PL system, demonstrating that this method obtains daylight outdoor PL images with only very little sunlight interference (PL signal component is >92%). Note that the image is blurry at the edges due to non-ideal custom-designed imaging optics. Figure 17(c) displays close-up images of the region, highlighted with a blue rectangle in figure 17(b), taken at 1 s and 50 s exposure time respectively. Both images demonstrate that high-definition outdoor PL images are possible with this method even with commercially relevant exposure times. Furthermore, the method can be used to detect series resistance-related issues in PV modules when combined with current extraction, for instance by changing the operating point of the PV

array via controlling the central inverter in a utility-scale PV power plant. The development of outdoor PL via UNBPF is currently at a proof-of-concept stage, but it is anticipated that further development of this technology may open the opportunity for routine and high-volume outdoor PL inspection via drones or ground-based vehicles.

6. Luminescence image quality, analysis, and fault detection

6.1. Image noise and signal-to-noise ratio

As discussed above, one of the key parameters determining the quality of the luminescence images is the SNR [83]. The SNR represents the ratio of the desired signal to the unwanted noise. There are multiple noise sources that affect luminescence-based measurements [84, 85] with the most important ones being:

- (a) *Dark current or thermal noise*, as resulting from thermal electrons in the camera sensor which are not related to the external photons. The number of thermal electrons increases linearly with exposure time and exponentially with sensor temperature, hence, to reduce the device's dark current noise, thermoelectric cooling is often employed in cameras used for luminescence imaging.
- (b) *Shot noise or Poisson noise* that results from statistical fluctuations in the number of electrons that are captured by a detector. Shot noise can be calculated as the square root of the number of electrons stored in a respective camera pixel. Therefore, taking images with increased capture time increases SNR as the signal increases linearly with exposure time while the Shot noise only increases as the square root of the exposure time.

Other noise sources originating from camera electronics include readout noise, amplifier noise, and quantisation noise. A good general introduction to image noise is provided in [86]. Typically, the dominating noise sources in luminescence images are thermal noise for nighttime measurements with long exposure times and Shot noise for daylight measurements where a small desired signal is competing with a large electron count in the pixel, stemming from unwanted reflected sunlight.

6.2. Imaging standard and consistency in image capture and processing

It is important for luminescence measurements to be performed and processed in a repeatable and consistent manner for reasons of comparability and to allow a subsequent image analysis. To ensure consistency in EL measurements, the technical standard IEC TS 60904-13:2018 provides a method to capture, process, and qualitatively and quantitatively interpret images of PV modules [87]. The standard is particularly important for outdoor luminescence imaging, which is intrinsically subjected to greater variability compared to indoor measurements due to constantly changing environmental conditions (strength and angle of the sunlight, angle of modules, distance between camera and module, cloud coverage, temperature changes, etc). Table 1 summarises some core differences between indoor and outdoor EL measurements.

To quantify EL measurement variation, an international inter-lab comparison round robin study was carried out among 17 laboratories across Europe and the USA, where EL images were processed according to the international standard IEC TS 60904-13:2018 [87]. One of the elementary parts of the quantitative analysis was to determine the cell's average EL intensity. The round robin study showed that without any correction, the average intensity of the tested cells varies by more than 15% (median EL intensity) between laboratories. With corrections applied according to the standard, the variation is decreased to 10%. The remaining error can be attributed to differences in camera calibration between laboratories, mainly as a result of the flatfield correction. With an automated camera calibration and image correction, the deviation between different laboratories could be further reduced to 3% [88]. This highlights the need for consistent image acquisition and image correction procedures, which is exacerbated in the case of outdoor luminescence measurements due to much more varied imaging conditions.

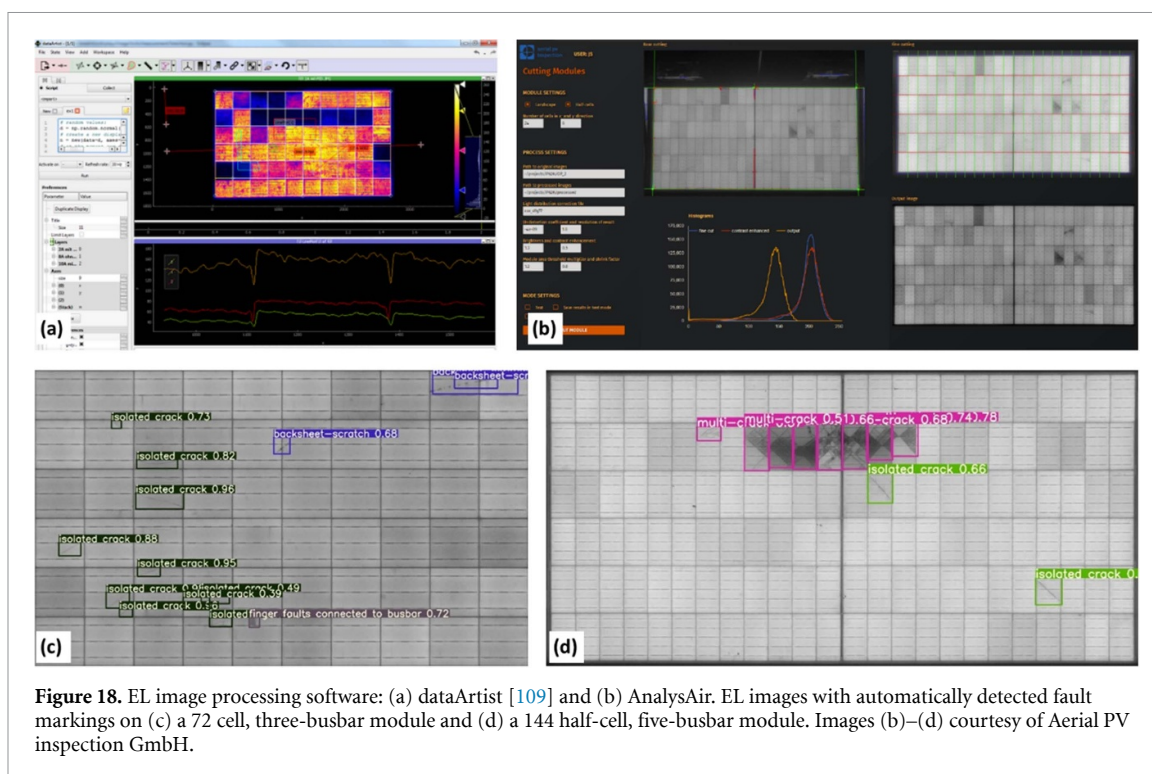
Note that it is critical when reporting the inspection results, to record the exact location of the modules in the PV installation. The modules can then be identified by combining information from the recorded position (geo position, height, and camera orientation), the installation layout plans, and the electrical string plans. In the future the availability of digital twins of PV plants can help in the geolocalisation and logging of measurements at string or module level.

6.3. Post-processing of outdoor luminescence images

Luminescence images taken outdoor are fundamentally affected by significant optical aberrations such as vignetting, perspective distortions, and lens distortions. Therefore, image post processing needs to automatically correct as many of these optical aberrations as possible [72, 89–94]. The next step is then to crop the module area as shown in figures 18(a) and (b) which display single module images after cropping.

Table 1. Selected differences between indoor and outdoor luminescence measurements.

Category	Indoor measurement	Outdoor measurement
Perspective distortion	Often much smaller or negligible due to the perpendicular angle between camera and module during imaging.	Often larger due to the use of tripods, drones, or similar means that may not be perpendicularly aligned to the modules.
Image blur	Negligible due to the stationary set-up.	Motion blur can occur in windy conditions and when moving imaging platforms are used (especially with long exposure times). Out-of-focus blur when lens not focused. Depth-of-field blur under perspective distortion especially with lenses of shorter focal length.
Ambient (stray) light	Little or none, due to measurement under a controlled dark room environment.	Substantial ambient light especially for daytime measurements where it needs to be reduced to acceptable levels via suitable bandpass filters and lock-in modulation. Light conditions can change substantially throughout the day and even during a single measurement (on cloudy days).
Temperature	Usually at room temperature (25 °C).	Varies depending on outdoor conditions (time of day, season, weather, etc).
Sensor technology used	Mostly (cooled) Si sensors due to lower cost and higher resolution.	Si sensors (only at night) or InGaAs sensors.
PV module conditions	Usually clean when measured.	Soiling, bird droppings, cables, left equipment, or wet spots are possible and affect the resulting image.



Finally, the image brightness and contrast need to be adjusted to enhance the detectability of certain fault types. Software that detects cell boundaries (cell segmentation) [95] supports further image processing and allows for automated feature/fault detection (see figures 18(c) and (d)). Two methods are common for processing luminescence videos: one automatically detects the sharpest frame of a PV module or area and selects this frame for further processing while discarding the other (blurrier) frames. Another method aligns and averages multiple frames or a PV module or area. While individual frames can be noisy, their average will have an f -times higher SNR, whereby f is the square root of the number of frames used for the average. Further processing includes perspective correction and possibly image enhancement.

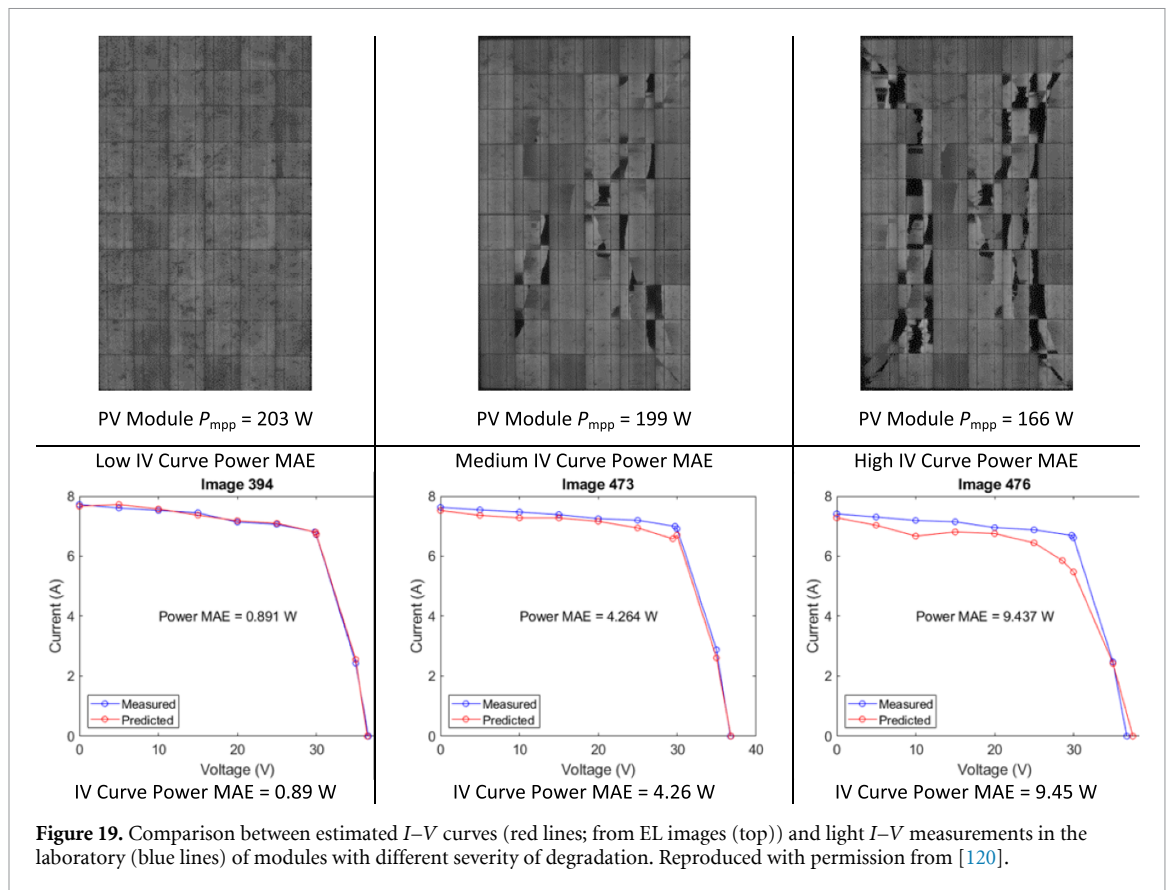


Figure 19. Comparison between estimated I - V curves (red lines; from EL images (top)) and light I - V measurements in the laboratory (blue lines) of modules with different severity of degradation. Reproduced with permission from [120].

To automatically and consistently identify faults and degradation modes in luminescence images, deep-learning methods such as convolutional neural networks (CNN) can be applied [37, 92, 95–101]. The CNNs are trained on thousands of images of various module types, where faults have been marked previously by human experts. This then enables the algorithms to automatically identify faults in new images, almost independent of cell sizes and module layouts (see figures 18(c) and (d)). The defects that are identified and classified by machine learning include micro-cracks, finger interruption, busbar corrosion, black core, cold soldering, shunts, and other defect types [33, 37, 96, 97, 102–106]. Another machine learning-based approach is the use of principal component analysis to categorise modules by features and faults [107].

Finally, after defect classification, the modules are sorted into quality categories with ratings based on the identified defect and degradation features. A widely used suitable rating scheme is the ‘MBJ Solar Module Judgment Criteria’ [108].

6.4. Quantifying power loss from luminescence images

Quantitative analysis of EL images has been widely studied in recent years [59, 88, 110–117] using various strategies. One method involves the determination of operating voltage and extraction of the electrical parameters of each cell [110–115, 118]. For example, Guo *et al* constructed a series of dark I - V curves for each individual solar cell from an EL image of a PV module [113]. Hence, the problems associated with each cell can be further investigated.

Recent studies have used machine learning to predict the PV module light I - V characteristics and subsequently the power loss from EL images [116, 117, 119, 120]. Bedrich *et al* developed an empirical method of quantitative EL analysis to estimate the relative power losses caused by PID which can accurately predict the power loss with a root mean square error of less than 3% [59]. With the ever-increasing volume of collected field luminescence images, this approach offers a powerful tool for qualitative and quantitative image analysis. As an example, Rodrigues Abreu *et al* propose a method to predict the module I - V curves from EL images using a deep learning algorithm [120]. As can be seen in figure 19, the method well predicts the I - V curves of three multicrystalline PV modules with different extents of cell cracking.

Quantitative luminescence image analysis has improved substantially in recent years, and it can be expected that the knowledge gained will subsequently be transferred to outdoor luminescence measurements of fielded PV modules.

Table 2. Comparison between various outdoor imaging methods.

Category	Outdoor EL	Outdoor luminescence with electrical modulation	Outdoor PL with optical string modulation	Outdoor PL without modulation	Outdoor PL with inverter switching
Commercial Readiness	Routinely used	Routinely used	Not yet in commercial use	Further technical development required	Further technical development required
Time of imaging	Night-time	Daytime or Night-time	Daytime	Daytime	Daytime
Technical requirements	Si camera (low cost) or InGaAs (high cost); Power supply with multiplexer switch and generator (or three-phase A/C power connection); Site preparation to connect equipment to PV strings	InGaAs camera (high cost); Power supply with DaySyBox and generator (or three-phase A/C power connection); Site preparation to connect equipment to PV strings	InGaAs camera (high cost); Battery powered wireless optical modulators	Cooled low-noise InGaAs camera (high cost); Sophisticated optical system with Ultra-narrow bandpass filter; Modules can be imaged at OC or with moderate current extraction	InGaAs camera (high cost); Means for wireless communication with the inverter
Image acquisition time	1–2 s (Si); 0.2–50 ms (InGaAs)	0.5–1 s	0.5–1 s	Currently 1–50 s	Currently about 27 s
Electrical connection to system required	Yes	Yes	No	No	No
Camera resolution	>10 M pixel (Si); 1.3 M pixel (InGaAs)	0.3 or 1.3 M pixel	0.3 or 1.3 M pixel	0.3 or 1.3 M pixel	0.3 or 1.3 M pixel
Throughput limitation	Site-preparation to connect to PV strings; Flight time if used with drones	Site-preparation to connect to PV strings; Flight time if used with drones	Movement of optical string modulators from string to string; Flight time if used with drones	Long image exposure time; Cannot be used from continuously moving test-bed	Long inverter switching time; Cannot be used from continuously moving test-bed

7. Comparison of different outdoor luminescence imaging methods

All outdoor luminescence methods that have been developed and are currently in use have their own advantages and drawbacks. Selection of the preferred inspection method for a given task needs to include consideration of various factors: (a) system design and accessibility, (b) imaging time (night or daylight imaging), (c) desired throughput and image resolution, (d) availability of trained personnel, (e) cost, (f) safety and environmental limitations, and (g) technology readiness level.

Some of the core requirements are identical for all methods, such as a tripod or other mechanical solution to mount the camera. Moving testbeds can also be used, such as basket crane vehicles, camera cranes, ground vehicles, or drones. In table 2, a comparison between the different methods is shown. The main features that distinguish the technologies are the time of use (daytime or night-time), the camera type (Si or InGaAs); the technological requirements; and site preparation requirements (electrical connections to strings). The camera resolution is also a feature of distinction but with modern InGaAs cameras available with 1.3 MP image resolution, this is becoming less of an issue. Both outdoor EL measurements and daylight luminescence measurements using the DaySy system are already in routine commercial use. Outdoor PL imaging using string modulation is technologically ready but not yet in commercial use. The two other methods, outdoor PL imaging without modulation (via UNBPF) and outdoor PL using inverter switching, have not yet reached the level where they can be useful for commercial deployment and hence require further technological development.

8. Summary and conclusions

Reliable inspection of solar power plants is required to ensure the installations are of high quality, safe to operate, and produce the maximum possible power for the longest possible plant life. Outdoor luminescence imaging of field-deployed PV modules provides module image data with unparalleled fidelity and is therefore the gold standard for assessing the quality, defect types, and degradation state of field-deployed PV modules. Several luminescence imaging methods have been developed and some of them are already routinely used to inspect solar power plants. The preferred inspection method to be used depends on the required image resolution, the defect types that need to be identified, cost, inspection throughput, technological readiness, and other factors. Due to the rich and detailed information provided by luminescence imaging measurements and modern image analysis methods, luminescence imaging is becoming an increasingly important tool for PV module quality assurance in PV power plants. Outdoor luminescence imaging can make valuable contributions to the commissioning, operation, and assessment of solar power plants prior to a change of ownership or after severe weather events. Another increasingly important use of these technologies is the end-of-life assessment of solar panels to enable a sustainable circular economy of the future.

Data availability statement

No new data were created or analysed in this study.

Acknowledgments

This work was kindly supported by the Australian Government through the Australian Renewable Energy Agency (ARENA) under the Grants 2017/01, 2019/CRD003 and 2020/RND016. O Kunz acknowledges the kind support by the Australian Centre for Advanced Photovoltaics (ACAP, Project RG212055-C). The views expressed herein are not necessarily the views of the Australian Government, and the Australian Government does not accept responsibility for any information or advice contained herein.

ORCID iDs

Oliver Kunz  <https://orcid.org/0000-0002-9300-0004>

Ziv Hameiri  <https://orcid.org/0000-0002-2934-4478>

References

- [1] Asmelash E and Prakash G 2019 Future of solar photovoltaic—a global energy transformation paper (IRENA) (available at: www.irena.org/publications/2019/Nov/Future-of-Solar-Photovoltaic)
- [2] World Economic Forum 2020 Solar is now 'cheapest electricity in history', confirms IEA (available at: www.weforum.org/agenda/2020/10/solar-energy-cheapest-in-history-iea-renewables-climate-change/)
- [3] Bellini E 2021 Saudi Arabia's second PV tender draws world record low bid of \$0.0104/kWh *PV Magazine* (available at: www.pv-magazine.com/2021/04/08/saudi-arabias-second-pv-tender-draws-world-record-low-bid-of-0104-kwh/)
- [4] I. International Energy Agency 2020 Renewables 2020—analysis and forecast to 2025 (available at: www.iea.org/reports/renewables-2020)
- [5] Kavlak G, McNerney J and Trancik J E 2018 Evaluating the causes of cost reduction in photovoltaic modules *Energy Policy* **123** 700–10
- [6] Green M A 2019 How did solar cells get so cheap? *Joule* **3** 631–3
- [7] Scully J 2021 Solar's 'unstoppable growth' puts sector on track for terawatt scale in 2022—SPE (PV Tech) (available at: www.pv-tech.org/solars-unstoppable-growth-puts-sector-on-track-for-terawatt-scale-in-2022-spe/)
- [8] Haegel N M et al 2019 Terawatt-scale photovoltaics: transform global energy *Science* **364** 836
- [9] International Energy Agency (IEA) 2022 Renewables 2021—analysis and forecast to 2026 (available at: www.https://iea.blob.core.windows.net/assets/5ae32253-7409-4f9a-a91d-1493ffb9777a/Renewables2021-Analysisandforecastto2026.pdf)
- [10] Lennon A, Lunardi M, Hallam B and Dias P R 2022 The aluminium demand risk of terawatt photovoltaics for net zero emissions by 2050 *Nat. Sustain.* **5** 357–63
- [11] Bogdanov D et al 2021 Low-cost renewable electricity as the key driver of the global energy transition towards sustainability *Energy* **227** 120467
- [12] Zhang Y, Kim M, Wang L, Verlinden P and Hallam B 2021 Design considerations for multi-terawatt scale manufacturing of existing and future photovoltaic technologies: challenges and opportunities related to silver, indium and bismuth consumption *Energy Environ. Sci.* **14** 5587–610
- [13] Creutzig F, Agoston P, Goldschmidt J C, Luderer G, Nemet G and Pietzcker R C 2017 The underestimated potential of solar energy to mitigate climate change *Nat. Energy* **2** 17140
- [14] Raworth K 2017 Exploring doughnut economics (available at: www.kateraworth.com/doughnut/)
- [15] Peters I M, Hauch J, Brabec C and Sinha P 2021 The value of stability in photovoltaics *Joule* **5** 3137–53
- [16] Makrides G, Zinsser B, Schubert M and Georghiou G E 2014 Performance loss rate of twelve photovoltaic technologies under field conditions using statistical techniques *Sol. Energy* **103** 28–42

- [17] Gupta V, Sharma M, Pachauri R and Babu K N D 2019 Impact of hailstorm on the performance of PV module: a review *Energy Sources A* **44** 1923–44
- [18] Muehleisen W et al 2017 Outdoor detection and visualization of hailstorm damages of photovoltaic plants *Renew. Energy* **118** 138–45
- [19] Morlier A, Siebert M, Kunze I, Mathiak G and Kontges M 2017 Detecting photovoltaic module failures in the field during daytime with ultraviolet fluorescence module inspection *IEEE J. Photovolt.* **7** 1710–6
- [20] Jahn U and Herteleer B 2022 Climate-specific O&M for PV power plants (PV-Tech) (available at: www.pv-tech.org/climate-specific-om-for-pv-power-plants/)
- [21] Aghaei M et al 2022 Review of degradation and failure phenomena in photovoltaic modules *Renew. Sustain. Energy Rev.* **159** 112160
- [22] Koester L, Lindig S, Louwen A, Astigarraga A, Manzolini G and Moser D 2022 Review of photovoltaic module degradation, field inspection techniques and techno-economic assessment *Renew. Sustain. Energy Rev.* **165** 112616
- [23] Tjengdrawira C, Moser D, Jahn U, Armansperg M V, Theologitis I-T and Heisz M 2017 PV investment technical risk management: best practice guidelines for risk identification, assessment and mitigation (available at: www.tuv.com/content-media-files/master-content/services/products/p06-solar/solar-downloadpage/solar_bankability_d5.8_best-practice-guidelines-for-risk-managment.pdf)
- [24] Farnung B, Ponzalan K and Moser D 2021 The impact of quality assurance measures in the early stage of a solar project (available at: www.pv-tech.org/the-impact-of-quality-assurance-measures-in-the-early-stage-of-a-solar-project/)
- [25] van der Heide A, Tous L, Wambach K, Poortmans J, Clyncke J and Voroshazi E 2021 Towards a successful re-use of decommissioned photovoltaic modules *Prog. Photovolt., Res. Appl.* **30** 910–20
- [26] Rahman M M, Khan I and Alameh K 2021 Potential measurement techniques for photovoltaic module failure diagnosis: a review *Renew. Sustain. Energy Rev.* **151** 111532
- [27] Deng R, Chang N and Green M 2021 Peer behaviour boosts recycling *Nat. Energy* **6** 862–3
- [28] Muehleisen W et al 2019 Scientific and economic comparison of outdoor characterisation methods for photovoltaic power plants *Renew. Energy* **134** 321–9
- [29] Chowdhury M S, Rahman K S, Chowdhury T, Nuthammachot N, Techato K, Akhtaruzzaman M, Tiong S K, Sopian K and Amin N 2020 An overview of solar photovoltaic panels' end-of-life material recycling *Energy Strateg. Rev.* **27** 100431
- [30] Jordan D C, Silverman T J, Wohlgenuth J, Kurtz S and VanSant K 2017 Photovoltaic failure and degradation modes *Prog. Photovolt., Res. Appl.* **25** 318–26
- [31] Herrmann W et al 2021 Qualification of photovoltaic (PV) power plants using mobile test equipment *IEA-PVPS T13-24:2021*
- [32] Sizkouhi A M M, Esmailifar S M, Aghaei M and Karimkhani M 2022 RoboPV: an integrated software package for autonomous aerial monitoring of large scale PV plants *Energy Convers. Manage.* **254** 115217
- [33] Deitsch S, Christlein V, Berger S, Buerhop-Lutz C, Maier A, Gallwitz F and Riess C 2019 Automatic classification of defective photovoltaic module cells in electroluminescence images *Sol. Energy* **185** 455–68
- [34] Rai-Roche S 2021 PV 2030: an automated and intelligent future for O&M (PV Tech) (available at: www.pv-tech.org/climate-specific-om-for-pv-power-plants/)
- [35] Filatoff N 2021 Drones and software loop the loop on autonomous, intelligent PV plant monitoring *PV Magazine* (available at: www.pv-magazine-australia.com/2021/10/18/drones-and-software-loop-the-loop-on-autonomous-intelligent-pv-plant-monitoring/)
- [36] Doll B et al 2021 Photoluminescence for defect detection on full-sized photovoltaic modules *IEEE J. Photovolt.* **11** 1419–29
- [37] Tang W, Yang Q and Yan W 2022 Deep learning-based algorithm for multi-type defects detection in solar cells with aerial EL images for photovoltaic plants *Compute. Model. Eng. Sci.* **130** 1423–39
- [38] Trupke T 2021 Thorsten Trupke's 2021 cherry award lecture (available at: www.acap.org.au/post/thorsten-trupke-s-2021-cherry-award-lecture)
- [39] Würfel P, Trupke T, Puzzer T, Schäffer E, Warta W and Glunz S W 2007 Diffusion lengths of silicon solar cells from luminescence images *J. Appl. Phys.* **101** 123110
- [40] Sproul A B and Green M A 1991 Improved value for the silicon intrinsic carrier concentration from 275 to 375 K *J. Appl. Phys.* **70** 846–54
- [41] Zafirovska I, Juhl M K, Ciesla A, Evans R and Trupke T 2019 Low temperature sensitivity of implied voltages from luminescence measured on crystalline silicon solar cells *Sol. Energy Mater. Sol. Cells* **199** 50–58
- [42] Dhouiab A and Filali S 1990 Operating temperatures of photovoltaic panels *Energy and the Environment* ed A A M Sayigh (Oxford: Pergamon) pp 494–8
- [43] Fuyuki T, Kondo H, Yamazaki T, Takahashi Y and Uraoka Y 2005 Photographic surveying of minority carrier diffusion length in polycrystalline silicon solar cells by electroluminescence *Appl. Phys. Lett.* **86** 262108
- [44] Trupke T, Bardos R A, Schubert M C and Warta W 2006 Photoluminescence imaging of silicon wafers *Appl. Phys. Lett.* **89** 044107
- [45] Trupke T, Mitchell B, Weber J W, McMillan W, Bardos R A and Kroeze R 2012 Photoluminescence imaging for photovoltaic applications *Energy Proc.* **15** 135–46
- [46] Ebner R, Kubicek B and Újvári G 2013 Non-destructive techniques for quality control of PV modules: infrared thermography, electro- and photoluminescence imaging *IECON 2013–39th Annual Conf. IEEE Industrial Electronics Society* pp 8104–9
- [47] Zafirovska I, Juhl M K, Weber J W, Wong J and Trupke T 2017 Detection of finger interruptions in silicon solar cells using line scan photoluminescence imaging *IEEE J. Photovolt.* **7** 1496–502
- [48] Kasemann M, Schubert M C, The M, Köber M, Hermlle M and Warta W 2006 Comparison of luminescence imaging and illuminated lock-in thermography on silicon solar cells *Appl. Phys. Lett.* **89** 224102
- [49] Trupke T, Pink E, Bardos R A and Abbott M D 2007 Spatially resolved series resistance of silicon solar cells obtained from luminescence imaging *Appl. Phys. Lett.* **90** 093506
- [50] Glatthaar M, Haunschild J, Kasemann M, Giesecke J, Warta W and Rein S 2010 Spatially resolved determination of dark saturation current and series resistance of silicon solar cells *Phys. Status Solidi* **4** 13–15
- [51] Dos Reis Benatto G A, Mantel C, Spataru S, Santamaria Lancia A A, Riedel N, Thorsteinsson S, Poulsen P B, Parikh H, Forchhammer S and Sera D 2020 Drone-based daylight electroluminescence imaging of PV modules *IEEE J. Photovolt.* **10** 872–7
- [52] Guada M, Moretón Á, Rodríguez-Conde S, Sánchez L A, Martínez M, González M Á, Jiménez J, Pérez L, Parra V and Martínez O 2020 Daylight luminescence system for silicon solar panels based on a bias switching method *Energy Sci. Eng.* **8** 3839–53
- [53] Bhoopathy R, Kunz O, Juhl M, Trupke T and Hameiri Z 2018 Outdoor photoluminescence imaging of photovoltaic modules with sunlight excitation *Prog. Photovolt., Res. Appl.* **26** 69–73

- [54] Koch S, Weber T, Christian S, Fladung A, Clemens P and Berghold J 2016 Outdoor electroluminescence imaging of crystalline photovoltaic modules: comparative study between manual ground—level inspections and drone—based aerial surveys *32nd European Photovoltaic Solar Energy Conf. and Exhibition* pp 1736–40
- [55] Doll B, Forberich K, Hepp J, Langner S, Buerhop-Lutz C, Hauch J A, Brabec C J and Peters I M 2022 Luminescence analysis of PV-module soiling in Germany *IEEE J. Photovolt.* **12** 81–87
- [56] de Oliveira A K V et al 2019 Low-cost aerial electroluminescence (aEL) of PV power plants *2019 IEEE 46th Photovoltaic Specialists Conf. (PVSC)* pp 532–7
- [57] Silverman T J, Deceglie M G, VanSant K, Johnston S and Repins I 2017 Illuminated outdoor luminescence imaging of photovoltaic modules *44th IEEE Photovoltaic Specialists Conf.* pp 3452–5
- [58] Stoicescu L, Reuter M and Werner J H 2016 DaySy reliably detects PID in daylight *32nd European PV Solar Energy Conf. and Exhibition*
- [59] Bedrich K G et al 2018 Quantitative electroluminescence imaging analysis for performance estimation of PID-influenced PV modules *IEEE J. Photovolt.* **8** 1281–8
- [60] Chai J, Bedrich K, Wang Y and Khoo Y S 2022 Quantified energy labs: technology (available at: <https://qe-labs.com/technology/>)
- [61] Stoicescu L, Reuter M and Werner J 2014 DaySy: luminescence imaging of PV modules in daylight *29th Eur. Photovoltaics Solar Energy Conf. Exhibition (Amsterdam, Netherlands)* pp 2553–4
- [62] Israil M and Kerm Y A G 2014 Non-destructive microcracks detection techniques in silicon solar cell *Phys. Sci. Int. J.* **4** 1073–87
- [63] Pingel S et al 2010 Potential induced degradation of solar cells and panels *IEEE Photovoltaic Specialists Conf.* pp 2817–22
- [64] Rahaman S A, Urmee T and Parlevliet D A 2020 PV system defects identification using Remotely Piloted Aircraft (RPA) based infrared (IR) imaging: a review *Sol. Energy* **206** 579–95
- [65] Jahn U and Herz M 2018 Review on infrared (IR) and electroluminescence (EL) imaging for photovoltaic field applications *IEA-Photovoltaic Power Systems Programme* (available at: https://iea-pvps.org/wp-content/uploads/2020/01/Review_on_IR_and_EL_Imaging_for_PV_Field_Applications_by_Task_13.pdf)
- [66] de Oliveira A K V, Aghaei M and R  ther R 2020 Aerial infrared thermography for low-cost and fast fault detection in utility-scale PV power plants *Sol. Energy* **211** 712–24
- [67] Parr A 1996 A national measurement system for radiometry, photometry, and pyrometry based upon absolute detectors *Technical Note (NIST TN)* (Gaithersburg, MD: National Institute of Standards and Technology)
- [68] Doll B, Pickel T, Schreer O, Zetzmann C, Hepp J, Teubner J, Buerhop C, Hauch J A, Camus C and Brabec C J 2019 High-throughput, outdoor characterization of photovoltaic modules by moving electroluminescence measurements *Opt. Eng.* **58** 1–13
- [69] Stoker L 2022 PVEL adds drone EL inspection services to offering with exclusive QE labs agreement (PV Tech) (available at: www.pv-tech.org/pvel-adds-drone-el-inspection-services-to-offering-with-exclusive-qe-labs-agreement/)
- [70] Colvin D J, Schneller E J, Horner G S, Gabor A M and Davis K O 2021 Evaluating impact on electroluminescence image quality and quantitative analysis using different camera technologies *2021 IEEE 48th Photovoltaic Specialists Conf. (PVSC)* pp 1057–61
- [71] Deceglie M G, Silverman T J, Johnston S W, Rand J A, Reed M J, Flottemesch R and Repins I L 2020 Light and elevated temperature induced degradation (LeTID) in a utility-scale photovoltaic system *IEEE J. Photovolt.* **10** 1084–92
- [72] Schlipf J and Fladung A 2018 Cell-level analysis of multi-megawatt PV plants *35th European Photovoltaic Solar Energy Conf. and Exhibition*
- [73] Delta Solar Solutions 2021 Delta launches M125HV Gen2 solar PV string inverter for large ground-mounted solar power plants (available at: <https://solarsolutions.delta-emea.com/en/Delta-Launches-M125HV-Gen2-String-Inverter-for-Large-Ground-mounted-Solar-Power-Plants-2226.htm>)
- [74] Bedrich K G 2022 Autonomous drone EL mapping for solar PV asset management *NREL PV Reliability Workshop (PVRW)*
- [75] ISO 1999 *Sampling procedures for inspection by attributes—part 1: sampling schemes indexed by acceptance quality limit (AQL) for lot-by-lot inspection* (International Organisation for Standardization) (available at: www.iso.org/obp/ui/#iso:std:iso:2859:-1:ed-2:v1:en)
- [76] Bhoopathy R, Kunz O, Juhl M, Trupke T and Hameiri Z 2019 Outdoor photoluminescence imaging of solar panels by contactless switching: technical considerations and applications *Prog. Photovolt., Res. Appl.* **28** 1–12
- [77] Kropp T, Berner M, Stoicescu L and Werner H 2017 Self-sourced daylight electroluminescence from photovoltaic modules *IEEE J. Photovolt.* **7** 1184–9
- [78] Solarzentrum Stuttgart GmbH 2019 DaySy measurement guide (available at: www.solarzentrum-stuttgart.com/uploads/file/DaySy_Measurement_Guide_current.pdf)
- [79] Vukovi   M, Eriksdatter H  iaas I, Jakovljevi   M, Svarstad Fl   A, Olsen E and Burud I 2022 Photoluminescence imaging of silicon modules in a string *Prog. Photovolt., Res. Appl.* **30** 436–46
- [80] Dos Reis Benatto G A et al 2017 Development of outdoor luminescence imaging for drone-based PV array inspection *2017 IEEE 44th Photovoltaic Specialist Conf. (PVSC)* pp 2682–7 (available at: <https://onlinelibrary.wiley.com/doi/10.1002/pip.3525>)
- [81] Kunz O, Rey G, Juhl M K and Trupke T 2021 High throughput outdoor photoluminescence imaging via PV string modulation *2021 48th IEEE Photovoltaic Specialists Conf. (PVSC)* pp 0346–50
- [82] Rey G, Kunz O, Green M and Trupke T 2022 Luminescence imaging of solar modules in full sunlight using ultranarrow bandpass filters *Prog. Photovolt., Res. Appl.* **30** 1115–21
- [83] Bedrich K G, Bliss M, Betts T R and Gottschalg R 2015 Electroluminescence imaging of PV devices: determining the image quality *2015 IEEE 42nd Photovoltaic Specialist Conf. (PVSC)* pp 1–5
- [84] Dussault D and Hoess P 2004 Noise performance comparison of ICCD with CCD and EMCCD cameras *Proc. SPIE* **5563**
- [85] Konnik M and Welsh J 2014 High-level numerical simulations of noise in CCD and CMOS photosensors: review and tutorial (<https://doi.org/10.48550/arXiv.1412.4031>)
- [86] Boncelet C 2009 *Image Noise Models* (Boston: Academic) ch 7, pp 143–67
- [87] Standard IEC TS 60904-13:2018 2018 *Photovoltaic Devices—Part 13: Electroluminescence of Photovoltaic Modules* (International Electrotechnical Commission) (available at: <https://webstore.iec.ch/publication/26703>)
- [88] Bedrich K et al 2018 1st international round Robin on EL imaging: automated camera calibration and image normalisation *35th European Photovoltaic Solar Energy Conf. and Exhibition*
- [89] K  lblin P, Bartler A and F  ller M 2021 Image preprocessing for outdoor luminescence inspection of large photovoltaic parks *Energies* **14** 2508
- [90] Bedrich K, Bokali   M, Bliss M, Topi   M, Betts T R and Gottschalg R 2018 Electroluminescence imaging of PV devices: advanced vignetting calibration *IEEE J. Photovolt.* **8** 1297–304

- [91] Mantel C, Villebro F, Parikh H R, Spataru S, Benatto G A D R, Sera D, Poulsen P B and Forchhammer S 2020 Method for estimation and correction of perspective distortion of electroluminescence images of photovoltaic panels *IEEE J. Photovolt.* **10** 1797–802
- [92] Otamendi U, Martinez I, Quartulli M, Olaizola I G, Viles E and Cambarau W 2021 Segmentation of cell-level anomalies in electroluminescence images of photovoltaic modules *Sol. Energy* **220** 914–26
- [93] Deitsch S, Buerhop-Lutz C, Sovetkin E, Steland A, Maier A, Gallwitz F and Riess C 2021 Segmentation of photovoltaic module cells in uncalibrated electroluminescence images *Mach. Vis. Appl.* **32** 84
- [94] Parikh H R et al 2018 Enhancement of electroluminescence images for fault detection in photovoltaic panels *2018 IEEE 7th World Conf. on Photovoltaic Energy Conversion (WCPEC) (A Joint Conf. 45th IEEE PVSC, 28th PVSEC & 34th EU PVSEC)* pp 447–52
- [95] Lin H-H, Dandage H K, Lin K-M, Lin Y-T and Chen Y-J 2021 Efficient cell segmentation from electroluminescent images of single-crystalline silicon photovoltaic modules and cell-based defect identification using deep learning with pseudo-colorization *Sensors* **21** 4292
- [96] Tang W, Yang Q, Xiong K and Yan W 2020 Deep learning based automatic defect identification of photovoltaic module using electroluminescence images *Sol. Energy* **201** 453–60
- [97] Demirci M Y, Bešli N and Gümüüşcü A 2021 Efficient deep feature extraction and classification for identifying defective photovoltaic module cells in Electroluminescence images *Expert Syst. Appl.* **175** 114810
- [98] Karimi A M, Fada J S, Liu J, Braid J L, Koyutürk M and French R H 2018 Feature extraction, supervised and unsupervised machine learning classification of PV cell electroluminescence images *2018 IEEE 7th World Conf. on Photovoltaic Energy Conversion (WCPEC) (A Joint Conf. 45th IEEE PVSC, 28th PVSEC & 34th EU PVSEC)* pp 418–24
- [99] Moradi Sizkouhi A, Aghaei M and Esmailifar S M 2021 A deep convolutional encoder-decoder architecture for autonomous fault detection of PV plants using multi-copters *Sol. Energy* **223** 217–28
- [100] Akram M W, Li G, Jin Y, Chen X, Zhu C, Zhao X, Khaliq A, Faheem M and Ahmad A 2019 CNN based automatic detection of photovoltaic cell defects in electroluminescence images *Energy* **189** 116319
- [101] Parikh H R, Buratti Y, Spataru S, Villebro F, Reis Benatto G A D, Poulsen P B, Wendlandt S, Kerekes T, Sera D and Hameiri Z 2020 Solar cell cracks and finger failure detection using statistical parameters of electroluminescence images and machine learning *Appl. Sci.* **10** 8834
- [102] Banda P and Barnard L 2018 A deep learning approach to photovoltaic cell defect classification *Proc. Annual Conf. South African Institute of Computer Scientists and Information Technologists* pp 215–21
- [103] Karimi A M, Fada J S, Hossain M A, Yang S, Peshek T J, Braid J L and French R H 2019 Automated pipeline for photovoltaic module electroluminescence image processing and degradation feature classification *IEEE J. Photovolt.* **9** 1324–35
- [104] Rahman M R U and Chen H 2020 Defects inspection in polycrystalline solar cells electroluminescence images using deep learning *IEEE Access* **8** 40547–58
- [105] Su B, Chen H, Chen P, Bian G, Liu K and Liu W 2021 Deep learning-based solar-cell manufacturing defect detection with complementary attention network *IEEE Trans. Ind. Inf.* **17** 4084–95
- [106] Zhao Y, Zhan K, Wang Z and Shen W 2021 Deep learning-based automatic detection of multitype defects in photovoltaic modules and application in real production line *Prog. Photovolt., Res. Appl.* **29** 471–84
- [107] Bordihn S, Fladung A, Schlipf J and Köntges M 2022 Machine learning based identification and classification of field-operation caused solar panel failures observed in electroluminescence images *IEEE J. Photovolt.* **12** 827–32
- [108] MJB Services GmbH, Germany 2019 MJB solar module judgment criteria, revision 3.4 (available at: www.solartester.eu/wp-content/uploads/2020/02/mjb-pv-module-judgement-criteria-3-4.pdf)
- [109] Bedrich K G, Bliss M, Betts T R and Gottschalg R 2016 Electroluminescence imaging of PV devices: camera calibration and image correction *2016 IEEE 43rd Photovoltaic Specialists Conf. (PVSC)* pp 1532–7
- [110] Köntges M, Siebert M and Hinken D 2009 Quantitative analysis of PV-modules by electroluminescence images for quality control *24th European Photovoltaic Solar Energy Conf.* pp 3226–31
- [111] Potthoff T, Bothe K, Eitner U, Hinken D and Köntges M 2010 Detection of the voltage distribution in photovoltaic modules by electroluminescence imaging *Prog. Photovolt., Res. Appl.* **18** 100–6
- [112] Li B, Stokes A and Doble D M J 2012 Evaluation of two-dimensional electrical properties of photovoltaic modules using bias-dependent electroluminescence *Prog. Photovolt., Res. Appl.* **20** 936–44
- [113] Guo S, Schneller E, Davis K O and Schoenfeld W V 2016 Quantitative analysis of crystalline silicon wafer PV modules by electroluminescence imaging *43rd IEEE Photovoltaic Specialists Conf.* pp 3688–92
- [114] Rajput A S, Ho J W, Zhang Y, Nalluri S and Aberle A G 2018 Quantitative estimation of electrical performance parameters of individual solar cells in silicon photovoltaic modules using electroluminescence imaging *Sol. Energy* **173** 201–8
- [115] Roy S and Gupta R 2019 Quantitative estimation of shunt resistance in crystalline silicon photovoltaic modules by electroluminescence imaging *IEEE J. Photovolt.* **9** 1741–7
- [116] Kumar V and Maheshwari P 2022 Advanced analytics on IV curves and electroluminescence images of photovoltaic modules using machine learning algorithms *Prog. Photovolt., Res. Appl.* **30** 880–8
- [117] Karimi A M, Fada J S, Parrilla N A, Pierce B G, Koyutürk M, French R H and Braid J L 2020 Generalized and mechanistic PV module performance prediction from computer vision and machine learning on electroluminescence images *IEEE J. Photovolt.* **10** 878–87
- [118] Puranik V E and Gupta R 2021 Novel quantitative electroluminescence method for detailed performance analysis of PID-s affected crystalline silicon PV module *IEEE J. Photovolt.* **11** 1470–8
- [119] Fada J S 2018 *Modeling Degradation of Photovoltaic Modules using Machine Learning of Electroluminescent Images* (Case Western Reserve University School of Graduate Studies, Case Western Reserve University School of Graduate Studies)
- [120] Rodrigues Abreu S, Buerhop-Lutz C, Doll B, Brabec C and Peters I M 2020 Predicting module I–V curves from electroluminescence images with deep learning *37th European Photovoltaic Solar Energy Conf. and Exhibition*